THESIS FOR THE DEGREE OF DOCTOR OF PHILOSOPHY

Hydrothermal Depolymerisation of Kraft Lignin

The Influence of Capping Agents and Residence Time

ANDERS AHLBOM

Department of Chemistry and Chemical Engineering

CHALMERS UNIVERSITY OF TECHNOLOGY

Gothenburg, Sweden 2023

Hydrothermal Depolymerisation of Kraft Lignin
The Influence of Capping Agents and Residence Time

ANDERS AHLBOM
ISBN 978-91-7905-808-1

Doktorsavhandlingar vid Chalmers tekniska högskola
Ny serie nr 5274
ISSN 0346-718X

Department of Chemistry and Chemical Engineering
Chalmers University of Technology
SE-412 96 Gothenburg
Sweden
Telephone + 46 (0)31-772 1000

Front cover:
The reactor used in this work, drawn by Frida Björklund.
Back cover:
Photograph by Johan Olsson.
Quote:
From the poem *I rörelse* by Karin Boye.

Printed by Chalmers Digitaltryck
Gothenburg, Sweden 2023

Hydrothermal Depolymerisation of Kraft Lignin

The Influence of Capping Agents and Residence Time

ANDERS AHLBOM

Department of Chemistry and Chemical Engineering

Chalmers University of Technology

Abstract

Lignin, the aromatic macromolecule found in wood and other lignocellulosic biomass, is envisioned as a future renewable source of aromatic compounds that can be used as, for example, chemicals, fuel additives and resins. A way in which this can be realised is by depolymerising the lignin once it has been isolated from the lignocellulosic biomass. Hydrothermal methods that employ water as a reaction medium are suggested as ways of accomplishing this. However, reactive fragments prone to repolymerisation, indeed char formation, are formed during depolymerisation, causing operational difficulties in the process as well as yield losses of the desired components. The suggestion has been made to add chemicals, i.e. capping agents, to scavenge the reactive components in order to mitigate these issues. Careful selection of reaction parameters, such as residence time and temperature, is also crucial for the process.

In this work, the depolymerisation of softwood kraft lignin has been investigated under hydrothermal conditions, with additions isopropanol, glycerol and guaiacol, to investigate their potential of functioning as capping agents. A customised batch reactor (99 cm^3) enabling swift heating of the reaction mixture was employed at 290-335 °C and 250 bar with low residence times (1-12 min).

The result of the hydrothermal depolymerisation of lignin was an aqueous suspension with a strong smoky odour. No apparent separate liquid organic phase was formed, although a char fraction precipitated. Characterisation of the products indicated a rapid depolymerisation of the lignin, since inter-unit ether linkages were cleaved, which was later followed by a slower repolymerisation. Additions of isopropanol, glycerol and guaiacol, reduced the weight average molecular weights (M_w) of the product fractions. Only isopropanol appeared to be able to reduce the amount of char formed from the lignin. Subsequent aftertreatment of the product would be required to obtain a usable product.

Keywords: *kraft lignin, depolymerisation, capping agents, isopropanol, guaiacol, glycerol, hydrothermal liquefaction*

”Nog finns det mål och mening i vår färd –

men det är vägen, som är mödan värd.”

Karin Boye

Preface

This dissertation is submitted as partial fulfilment of the degree of Doctor of Philosophy. The work was conducted primarily at the Division of Forest Products and Chemical Engineering (SIKT) at the Department of Chemistry and Chemical Engineering at Chalmers University of Technology in Gothenburg, Sweden, between September 2018 and March 2023, under the supervision of Professor Hans Theliander and Associate Professor Merima Hasani. Substantial work was carried out at Aalborg University in Esbjerg, Denmark, under the supervision of Associate Professor Marco Maschietti and assistance from Associate Professor Rudi Nielsen. The work was funded by the Swedish Energy Agency.

Anders Ahlbom

March 2023, Gothenburg

List of publications

This thesis is based on the following appended papers:

Paper I: **Using Isopropanol as a Capping Agent in the Hydrothermal Liquefaction of Kraft Lignin in Near-Critical Water.** Ahlbom A, Maschietti M, Nielsen R, Lyckeskog H, Hasani M, Theliander H. *Energies*. 2021; 14(4):932. https://doi.org/10.3390/en14040932

Paper II: **Towards understanding kraft lignin depolymerisation under hydrothermal conditions.** Ahlbom A, Maschietti M, Nielsen R, Hasani M, Theliander H. *Holzforschung*. 2021;76(1):37-48. https://doi.org/10.1515/hf-2021-0121

Paper III: **On the hydrothermal depolymerisation of kraft lignin using glycerol as a capping agent**. Ahlbom A, Maschietti M, Nielsen R, Hasani M, Theliander H. *Holzforschung*. 2023; https://doi.org/10.1515/hf-2022-0146

Paper IV: **Using Guaiacol as a Capping Agent in the Hydrothermal Depolymerisation of Kraft Lignin.** Ahlbom A, Maschietti M, Nielsen R, Hasani M, Theliander H. *Submitted Manuscript.*

Contribution report

Paper I: **Main author.** AA planned the experiments together with HT, MM and MH and performed them with MM and RN. AA was the main person responsible for the ensuing characterisations, and the results were evaluated in collaboration with the co-authors. AA drafted the manuscript and revised it after receiving co-author feedback.

Paper II: **Main author.** AA planned the experiments together with HT, MM and MH and performed them with MM and RN. AA was the main person responsible for the ensuing characterisations, and the results were evaluated in collaboration with the co-authors. AA drafted the manuscript and revised it after receiving co-author feedback.

Paper III: **Main author.** AA planned the experiments together with HT, MM and MH and performed them with MM and RN. AA was the main person responsible for the ensuing characterisations, and the results were evaluated in collaboration with the co-authors. AA drafted the manuscript and revised it after receiving co-author feedback.

Paper IV: **Main author.** AA planned the experiments together with HT, MM and MH and performed them with MM and RN. AA was the main person responsible for the ensuing characterisations, and the results were evaluated in collaboration with the co-authors. AA drafted the manuscript and revised it after receiving co-author feedback.

Results related to this work have also been presented at the following conferences

(i) ***Hydrothermal kraft lignin depolymerization with glycerol as a capping agent*** Anders Ahlbom, Marco Maschietti, Rudi Nielsen, Merima Hasani, Hans Theliander. *Lignin Conference 2022* hosted by LignoCOST, Wageningen, The Netherlands, May 31-June 3, 2022 (Poster)

(ii) ***Using isopropanol as a capping agent in hydrothermal liquefaction of kraft lignin*** Anders Ahlbom, Marco Maschietti, Rudi Nielsen, Merima Hasani, Hans Theliander. *16th European Workshop on Lignocellulosics and Pulp (EWLP)*, Gothenburg, Sweden, June 28 -July 1, 2022 (Poster)

(iii) ***Swift Kraft lignin depolymerisation under hydrothermal conditions*** Anders Ahlbom, Marco Maschietti, Rudi Nielsen, Merima Hasani, Hans Theliander *International Bioenergy & Bioproducts Conference (IBBC)* hosted by TAPPI, Providence, Rhode Island, USA, October 30-November 2, 2022 (Oral presentation)

List of abbreviations

AAS	Atomic Absorption Spectroscopy
AC	Activated Carbon
ASO	Acid Soluble Organics
ATR	Attenuated Total Reflectance
BCD	Base Catalysed Depolymerisation
BHT	Butylated Hydroxytoluene
C-C	Carbon-Carbon bond
CHNS	Elemental analysis of Carbon, Hydrogen, Nitrogen and Sulphur
C-O	Carbon-Oxygen bond
co-FCC	Coprocessing in Fluid Catalytic Cracking
DEE	Diethyl Ether
DMSO	Dimethyl Sulphoxide
DMSO-*d6*	Deuterated Dimethyl Sulfoxide
EtOAc	Ethyl Acetate
EtOH	Ethanol
EWG	Electron Withdrawing Group
FID	Flame Ionisation Detector
FTIR	Fourier Transform Infrared Spectroscopy
GC	Gas Chromatography
GPC	Gel Permeation Chromatography
HDN	Hydrodenitrogenation
HDO	Hydrodeoxygenation
HDS	Hydrodesulphurisation
HMBC	Heteronuclear Multiple Bond Correlation (Spectroscopy)
HSQC	Heteronuclear Single Quantum Coherence (Spectroscopy)
HW	Hardwood
ICP-OES	Inductively Coupled Plasma - Optical Emission Spectrometry
IST	Internal Standard
MeOH	Methanol
MS	Mass Spectrometry
M_w	Weight Average Molecular Weight
MIBK	Methyl Isobutyl Ketone
NMR	Nuclear Magnetic Resonance (Spectroscopy)
P&I	Piping and Instrumentation
PS	Precipitated Solids
RI	Refractive Index
RSD	Relative Standard Deviation
SW	Softwood
TCD	Thermal Conductivity Detector
TMS	Tetramethylsilane
THF	Tetrahydrofuran
UV	Ultraviolet Light
VGO	Vacuum Gas Oil

Contents

1 Introduction

The pursuit of alternatives to fossil resources has led to a huge interest in renewable resources, for use as both materials and energy. Lignocellulosic materials such as wood are at the heart of this interest due to the abundance and distribution of trees and plants over the globe. Comprised mainly of cellulose, hemicelluloses and lignin, they have long been used as a source of fibres for board, paper, textiles and cellulose derivatives. These applications exploit the carbohydrate fractions of the lignocellulosic raw material. The lignin part, however, which forms 15-40 % of the dry weight of plant material, is still used mainly as a low-grade fuel, mostly in the recovery of chemicals in pulping processes (Ragauskas *et al.* 2014). However, lignin has a multitude of aromatic functionalities in its chemical structure, giving it good potential of becoming the largest renewable source of aromatics in the future (Balakshin *et al.* 2021). As such, it is desirable to use this widespread material but, in order to harness these aromatics, isolation is required: first of the lignin from the lignocellulosic biomass and then of the aromatics from the macromolecular structure of the lignin.

Lignin, in the form of lignosulphonates from sulphite pulp mills, has been extracted since the 1930s and used as, for example, dispersants and binders (McCarthy and Islam 2000). However, the main chemical process that treats lignin globally is the kraft pulping process, which is used to produce more than 90 % of chemical pulps in the world (Schutyser *et al.* 2018). A common estimation is that, from each tonne of kraft pulp produced, 0.42 tonnes of kraft lignin is liberated to the black liquor, the cooking liquor in the process (Gellerstedt *et al.* 2013). With ca. 148 million tonnes of kraft pulp being produced in 2021 (FAO 2021), an estimate of about 63 million tonnes of kraft lignin are processed every year in chemical pulping mills: the amount

of kraft lignin handled annually is therefore huge. The lignin produced in the kraft process is used as fuel providing energy and closing the chemical recovery cycle. With the increasing energy efficiency of pulp mills, all the latent energy recovered when combusting the lignin in the black liquor is not needed in the kraft process, which opens up the possibility of extracting kraft lignin from the black liquor by, e.g., the LignoBoost process (Dessbesell *et al.* 2020). As such, lignin then becomes available in the form of a brown powder.

The kraft pulping process not only degrades the lignin as it is removed from the biomass but also causes condensation in its structure, causing it to become recalcitrant (Schutyser *et al.* 2018). Even so, kraft lignin has been proposed for use as a raw material in many applications, such as adhesives, resins, carbon fibres, solid and liquefied fuel, or as a source of various aromatic compounds, not the least due to its large scale handling and established methods of recovery (Balakshin *et al.* 2021; Dessbesell *et al.* 2020; Lawoko and Samec 2023; Otromke *et al.* 2019a). Kraft lignin may be characterised as a heterogeneous macromolecule, with reported weight average molecular weight (M_w) in the range of 2570-42900 Da (Gellerstedt 2015; Sulaeva *et al.* 2017) and 14000-16000 Da (Zinovyev *et al.* 2018). The aromatic functionalities in lignin can be accessed by breaking down the structure into smaller entities, a process referred to as depolymerisation. Multiple ways of achieving this have been explored: both pyrolytic, reductive and oxidative pathways (Pandey and Kim 2011). Furthermore, hydrothermal methods, using water as the reaction medium can be employed, both above and below the critical point of water, i.e. at sub and supercritical reaction conditions (Dunn and Hobson 2016). The use of water open hydrolytic reaction pathways (Brand *et al.* 2014; Cheng *et al.* 2012).

Owing to the complexity of lignin, a multitude of reaction mechanisms are in play when the various bonds in its molecules are broken during depolymerisation. Reactive intermediates are formed that may react further, resulting in, at the very least, a partial repolymerisation which competes with the depolymerisation itself (Schutyser *et al.* 2018). With the goal being to depolymerise the lignin, such repolymerisation is naturally undesirable. It has been suggested that such repolymerisation can be mitigated by the addition of capping agents which trap the reactive species (Belkheiri *et al.* 2018a; Roberts *et al.* 2011). Furthermore, reaction parameters, such as temperature and residence time in the reactor are important since it appears that repolymerisation occurs at a slower rate than depolymerisation (Bobleter and Concin 1979). Controlling repolymerisation, by either adding a capping agent or adjusting other reaction parameters, therefore is a step towards allowing hydrothermal depolymerisation to advance as a way of valorising kraft lignin and utilising the aromatic structures therein.

1.1 Objective

The objective of this work is to investigate the capping effects of different alcohols on the depolymerisation of kraft lignin under hydrothermal conditions in subcritical water. The underlying hypothesis is that the alcohols will react with reactive components formed from the lignin and thereby mitigate repolymerisation of the products.

The effect of residence time is also investigated, and is based on the assumption that the depolymerisation of kraft lignin under hydrothermal conditions, in subcritical water, is a rapid process.

1.2 Scope

The hydrothermal treatment of softwood kraft lignin in water at 250 bar under subcritical temperatures of 290-335 °C and with the addition of a capping agent is evaluated by investigating the yields of the products, changes in their molecular weights and structures, along with their elemental compositions and functional groups. The capping agents investigated are the alcohols isopropanol, glycerol and guaiacol, which are added to an alkaline reaction mixture.

The effect of residence time is also investigated with the addition of these three alcohols. Here, the focus is on short residence times, i.e. 1-12 min.

1.3 Outline

The thesis is based on four papers, all of which are appended. Chapter 2 covers the basics of lignin chemistry and its isolation from biomass; different ways of depolymerising lignin are also outlined. In Chapter 3, the experimental set-up used for the depolymerisation of lignin is explained, and the fractionation of the products and their subsequent characterisation are described. Results and discussions of the kraft lignin depolymerisation are submitted in Chapter 4, which is followed by Chapter 5 which reports the conclusions that are drawn. Finally, some suggestions for future work are presented in Chapter 6.

2
Background

A brief introduction to lignin and its isolation from biomass begins this chapter. Technical lignins, are described here: for those such as milled wood lignin and various types of enzymatically-liberated lignins obtained on a smaller scale for research purposes, see Schutyser *et al.* (2018). A brief overview of methods used in the depolymerisation of lignin then follows.

2.1 Lignin

Lignin is an aromatic macromolecule found in lignocellulosic biomasses such as wood and grasses. It is located both within the different layers of the cell walls as well as in between the cells in the so-called middle lamellae. Indeed, it is often referred to as the glue between fibres, as well as between the fibrils within the fibre wall. Lignin thereby not only provides strength to the cell wall but also to the entire lignocellulosic structure. Furthermore, it renders both microbial and water resistance to the plant (Henriksson 2009). Lignin thus serves many different, and important, purposes.

Lignin forms the second largest fraction of the lignocellulosic biomass, after cellulose. Depending on the species, the amount of lignin in wood varies, with softwoods having more lignin than hardwood: examples of typical compositions of various types of wood are shown in Table 1 (Henriksson *et al.* 2009).

Table 1: Typical compositions of temperate softwood and hardwood (adapted from Henriksson et al. (2009)).

Wood type	Cellulose (%)	Hemicelluloses (%)	Lignin (%)
Temperate softwood	40-45	25-30	25-30
Temperature hardwood	40-45	30-35	20-25

2.1.1 Structure and formation of lignin

In plant cells, lignin is mainly synthesised from three different monolignols: *p*-coumaryl alcohol, coniferyl alcohol and sinapyl alcohol, shown in Figure 1. These main monolignols are also accompanied by other monomers in lower concentration, such as conifer aldehyde and ferulic acid (Henriksson 2009). The proportions of monolignols present in the lignin structure depend on the plant species as well as location in the plant (Mottiar *et al.* 2016).

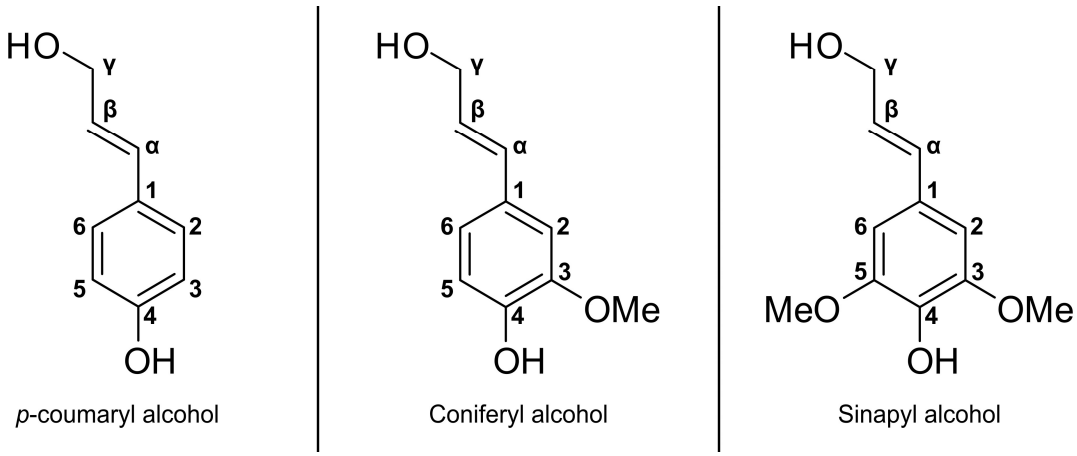

Figure 1: The three most common monolignols found in lignin (adapted from Mottiar et al. (2016)).

Softwood lignin is typically polymerised from coniferyl alcohol (>95 %), with small amounts of *p*-coumaryl alcohol (<5 %); there is no, or just trace amounts of, sinapyl alcohol in softwood lignin (Dimmel 2010; Henriksson 2009). Hardwood lignins contain all types of monolignols: both coniferyl and sinapyl alcohol, and some *p*-coumaryl alcohol. The monolignol *p*-coumaryl is primarily present in grasses, which also contain coniferyl and sinapyl alcohol as well (Henriksson 2009). When the monolignols are incorporated in the lignin structure, they are denoted H, G and S for their respective content of *p*-hydroxyphenyl (H), guaiacyl (G) and syringyl (S) moieties (Mottiar *et al.* 2016).

Lignin polymerises via a radical-induced pathway initiated by oxidation of the monolignols with laccase and peroxidase enzymes in the plant cell walls (Mottiar *et al.* 2016). The monolignols are bound together in the lignin by both ether (C-O) and carbon-carbon (C-C) bonds. Resonance stabilisation of charges guides the radical polymerisation so that certain specific inter-unit linkages form (Dimmel 2010); bonds thus form between the radicals shown in Figure 2. The nomenclature of these bonds follows the numbering shown in Figure 1. Since the quantity of monolignols in different types of wood varies, the amount of the types of bonds present also differs. Polymerisation through the radical coupling of oxidised monolignols causes a random distribution of the bonds, resulting in a final lignin structure that is amorphous (McCarthy and Islam 2000).

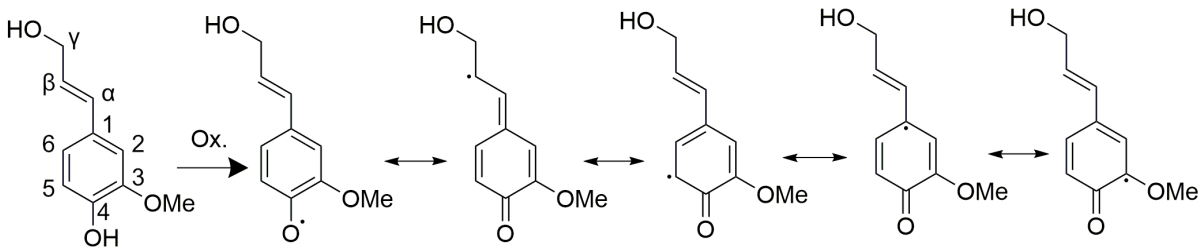

Figure 2: Resonance-stabilised radicals of coniferyl alcohol in the synthesis of lignin (adapted from Henriksson (2009) and *Mottiar et al. (2016)). Ox.: Oxidation performed using laccases or peroxidases.*

As mentioned above, different bonds will form depending on the monolignol being polymerised, because access to positions 3 and 5 on the aromatic ring differs between the monolignols. While *p*-coumaryl alcohol has no methoxy group attached to the aromatic ring, coniferyl alcohol has one and sinapyl alcohol two: the latter two methoxy groups block positions 3 and 5 on the aromatic ring. Consequently, lignin comprised mainly of sinapyl alcohol (S-units) cannot form bonds on positions 3 and 5, which means they are more prone to forming, e.g., β-O-4' bonds than lignin with a lot of coniferyl alcohol, i.e. softwood lignin (Dimmel 2010; Ragauskas *et al.* 2014). The C-C bonds are stronger than the C-O bonds, so the reactivity of lignin sourced from hardwood and softwood differs (Mottiar *et al.* 2016).

Lignin is thoroughly incorporated into the lignocellulosic structure and, in order to study it, must therefore be extracted (Dimmel 2010). Although even mild processes of extraction cause its structure to change, painstaking work undertaken by lignin chemists over the last century and a half (reviewed e.g. by Adler, and McCarthy and Islam (Adler 1977; McCarthy and Islam 2000)) has nevertheless resulted in information being obtained of typical inter-unit linkages present in lignin, shown in Figure 3. This knowledge is integral for the understanding of lignin and its isolation from lignocellulosic biomass.

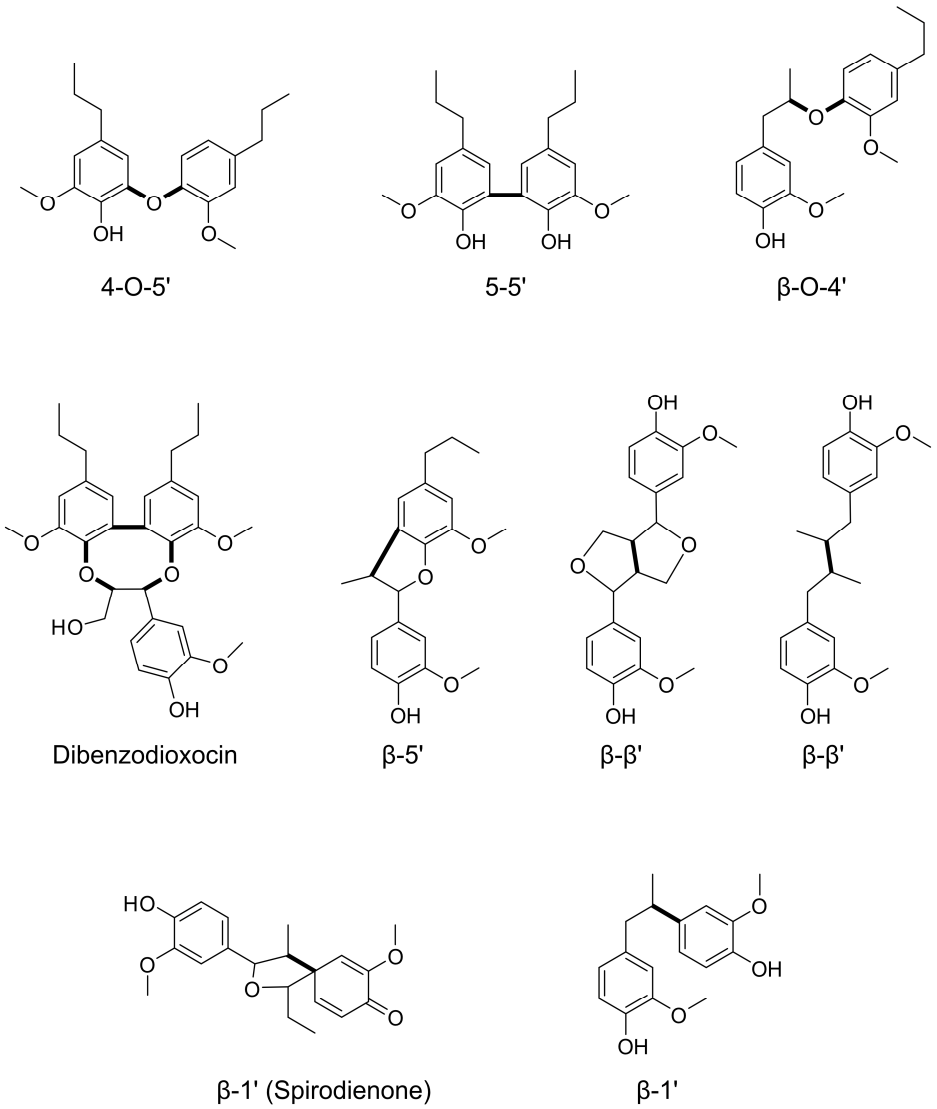

Figure 3: Typical inter-unit linkages in lignin (adapted from Dimmel (2010) and Henriksson (2009)). Side chain hydroxyl groups are omitted for clarity. All bonds shown are formed exclusively from coniferyl alcohol with one methoxy group on the aromatic ring.

2.1.2 Separating lignin from lignocellulosic biomass

The pulping industry has developed several methods for extracting lignin from lignocellulosic biomass (usually wood) by employing various chemical processes, known as pulping, to liberate the fibres. These seek to solubilise the lignin in the pulping liquor, thereby allowing it to be removed. This is achieved by reactions breaking the lignin structure, typically the more easily cleaved ether bonds such as β-O-4', which both lowers the molecular weight and frees phenolic groups that help solubilise the lignin. Also, functional groups that aid in solubilising the lignin can be incorporated in the lignin structure, as in the sulphite process (Lora 2008). This alters the structure of lignin, compared to its native structure in wood which contains many bonds between the monolignols that compose the lignin, as well as in between lignin and carbohydrates. Moreover, during the pulping process, lignin also condenses (to a certain extent) into a more recalcitrant form, with a higher degree of more stable C-C along with a lower number of weaker ether bonds (Schutyser *et al.* 2018).

2.1.3 Technical lignins

Technical lignins refer to side products isolated by industrial processes: chemical pulping or acid hydrolysis (Berlin and Balakshin 2014; Otromke *et al.* 2019c). While huge amounts of lignin are processed annually, it does not mean it is available on the market because the majority is incinerated for energy, primarily in the kraft process (Dessbesell *et al.* 2020). Usage of these lignins has been, and remains, a sought-after goal. Lignin, thus, remains underutilised, and Bruijnincx *et al.* note that most lignin applications have not advanced beyond pilot or laboratory scale (Bruijnincx *et al.* 2016). A brief introduction to technical lignins is given below.

2.1.3.1 Lignosulphonates

Lignosulphonates are the lignin products of sulphite pulping, which is performed at low pH even though it is possible to run at neutral or even alkaline conditions. Sulphite and bisulphite ions are used, with sodium, calcium, magnesium or ammonium ions as counter ions (Gellerstedt 2009). Hydrolysis serves to partly break the lignin structure and aid in dissolution (Saake and Lehnen 2007). Furthermore, sulphonate groups are incorporated on the reactive benzylic carbon (C_α) position in the lignin monomers, thereby making the lignin soluble in water. However, condensation might also occur on the C_α with aromatic rings, which hampers dissolution of the lignin (Gellerstedt and Henriksson 2008).

Not only lignin but also carbohydrates are liberated from lignocellulosic biomass during the sulphite pulping process. These sugars can be fermented into ethanol, whereafter the lignin may be isolated. However, the sulphonate groups make the lignosulphonates soluble at all pH levels. They are therefore not usually isolated by precipitation but instead by membrane filtration and evaporation, followed by spray drying, to remove residual water (Gellerstedt *et al.* 2013; Lora 2008).

Sulphite pulping, which dominated the chemical pulping industry for a long time, lost it dominance to kraft pulping in the 1950s, owing to the versatility of the latter process in terms of feedstock (Lora 2008). Also, the kraft process provides stronger pulp and an efficient chemical recovery process and so, today, sulphite pulping represents only a few percent of the total chemical pulping. However, most of the technical lignin used are lignosulphonates. The total lignin market as of 2018 was 1.65 Mt/y, 79 % of which were lignosulphonates (Dessbesell *et al.* 2020). These lignosulphonates find uses as e.g. dispersants and binders (Lora 2008).

2.1.3.2 Kraft lignin

Alkaline lignin can be procured from kraft and soda pulping processes, both of which use OH^- as an active cooking chemical. In the kraft process, HS^- is also employed because it gives a more efficient depolymerisation of the lignin compared to soda cooking, as phenolic units can be depolymerised more easily via quinone methides. In soda cooking, which only uses OH^-, predominately non-phenolic bonds are cleaved (Gellerstedt 2009). The more efficient lignin depolymerisation that occurs in kraft cooking allows the digestion time to be reduced, which ultimately yields a pulp of higher quality because peeling reactions and alkaline hydrolysis have less time to degrade the carbohydrates. Indeed, the term *kraft* is German for *strength*, which relates to the stronger pulp fibres produced by this process compared with sulphite pulps

(Saake and Lehnen 2007). The kraft pulping process, however, causes the lignin to condense, which makes further depolymerisation a challenge (Schutyser *et al.* 2018).

The liquor that remains after cooking kraft pulp is an aqueous mixture comprised of components from degraded carbohydrates, dissolved lignin and residual cooking chemicals, and is called black liquor. The cooking chemicals are recovered from the black liquor through evaporation and incineration (the latter performed in a recovery boiler), which reduces the sulphur compounds in the black liquor and enables the cooking chemicals to be recycled. Besides producing a salt smelt that is used for making new cooking chemicals, the recovery boiler also generates steam that is used as a heating medium in several units in the kraft process, e.g. the digester, evaporation plant and driers. Alternatively, with increased energy efficiency of mills, and de-bottlenecking of the often-limiting recovery boiler, kraft lignin can be recovered from the black liquor instead of being incinerated (Zhu *et al.* 2014). This requires that not only the energy balance but also the Na/S balance of the mill are taken into consideration (Gellerstedt *et al.* 2013).

Isolating kraft lignin from black liquor is achieved by precipitation, filtering and subsequent washing. Kraft lignin contains some sulphur (ca. 2-3 %), although less than lignosulphonates. Commercial technology for isolating kraft lignin includes the LignoBoost process, which produces a kraft lignin with low contents of ash and residual sugars (Gellerstedt *et al.* 2013; Theliander 2008; Zhu *et al.* 2014).

The annual production of isolated kraft lignin in 2018 was 265 kt/y, representing 16 % of the total market for technical lignin. Of the large amount of kraft lignin handled in existing pulping mills, the potential of producing 3.5-14 Mt/y was estimated by Dessbesell *et al.* (2020). It is interesting to note that this estimate takes into account the energy needs of the pulping mills and exceeds by several times the current production of kraft lignin. There are thus good possibilities to produce more kraft lignin with the existing pulping infrastructure.

2.1.3.3 Organosolv lignin and acid hydrolysis lignins

Pulping biomass in an organic solvent and water mixture gives so-called organosolv lignin. Normally, organic solvents with low boiling points, e.g. methanol and ethanol, are used because they make downstream separation from the water in the pulping liquor easier (Schutyser *et al.* 2018). During the pulping process, acetic acid is released from hemicelluloses in the biomass, which lowers the pH and thus facilitates delignification. Acid can also be added to the process; indeed, organosolv pulping can be carried out in formic or acetic acid (Saake and Lehnen 2007). Organosolv lignin is not produced in large amounts; no industrial scale set-up has been installed even though pilot units have been in operation (and later going bankrupt), such as the unit producing Alcell lignin (Bruijnincx *et al.* 2016; Dessbesell *et al.* 2020). Soda lignin and lignins from the hydrolysis of biomass used in the production of ethanol constitute the final 5 % of the technical lignin market (Dessbesell *et al.* 2020).

Lastly, it can also be noted that much lignin historically has been produced as a by-product in the acid hydrolysis process that is used to make ethanol from wood (McCarthy and Islam 2000). Such ethanol was used in the production of butadiene rubber, fodder yeast, furfural and xylitol in, e.g., the Soviet Union (Rabinovich 2010).

2.2 Methods of depolymerising lignin

The depolymerisation of lignin has been the subject of research for a long time, not least for analytical purposes where the selective degradation of lignin was integral in investigating its structure (Adler 1977; McCarthy and Islam 2000). Later work has been directed at depolymerisation using a range of different methods with the intent of valorising the lignin for use e.g. as adhesives, resins, carbon fibres, solid and liquefied fuel, or as a source of various aromatic compounds (Balakshin *et al.* 2021; Dessbesell *et al.* 2020; Lawoko and Samec 2023). These methods each have their own merits and drawbacks; they are presented briefly below.

2.2.1 Hydroprocessing

Employing hydrogen in lignin treatment opens many possibilities, e.g. depolymerisation and oxygen removal. Moreover, it can reduce the amount of char produced in pyrolysis (Zakzeski *et al.* 2010). Not only hydrogen gas but also hydrogen-donating solvents, such as tetralin, formic acid and isopropanol, can provide the hydrogen required for hydroprocessing (Kim *et al.* 2014; Pandey and Kim 2011).

The similarity between the structures of lignin and coal has meant that research on the liquefaction of coal, such as the work of Nobel Laureates Friedrich Bergius and Carl Bosch, could be adapted to lignin in the Noguchi process (Jensen *et al.* 2018; Zakzeski *et al.* 2010). High pressure reaction systems, with H_2 added together with a catalyst, depolymerised lignin through hydrogenolysis in a recirculated phenol and lignin tar mixture. Such hydrogenolysis is normally achieved by heterogeneous catalysis (Cao *et al.* 2018).

Hydroprocessing is not only used for depolymerisation but also for removing heteroatoms, such as oxygen, in a process called hydrotreatment. Thus, bio-oils produced from lignin can be after-treated with hydrodeoxygenation (HDO) processes that lower the oxygen content of the bio-oils and make them more suitable for use as fuel (Lawoko and Samec 2023). This mimics conventional petroleum processing, which employs catalytic hydrodesulphurisation (HDS) and hydrodenitrogenation (HDN) to remove sulphur and nitrogen, respectively (Zakzeski *et al.* 2010). However, issues concerning stability, poisoning and deactivation of the catalysts, along with the diverse reactions producing a multitude of low-molecular weight species, present great technical challenges (Ragauskas *et al.* 2014). Furthermore, the excessive water produced as a side product can be detrimental to the catalyst support (Lange 2015). Suggestions for overcoming these challenges include the use of bimetallic catalysts and alternative supports for the catalysts (Ragauskas *et al.* 2014).

Hydrogenation of lignin removes unsaturated aliphatic moieties in the lignin structure, even though saturation of the aromatic ring is also possible (Zakzeski *et al.* 2010). Careful tuning of the reaction is necessary to ensure that the aromatic rings desirable in lignin are not lost.

2.2.2 Oxidation

Oxidative methods employed to depolymerise lignin include commercial processes, such as bleaching of pulp and the production of vanillin from lignosulphonates, as well as emerging technologies for low temperature treatments of lignin that yield highly functionalised chemicals (Abdelaziz *et al.* 2019a; Henriksson 2009). The possibility of producing vanillin from spent sulphite liquors was described by Pollacsek as early as in 1898 (McCarthy and Islam 2000).

Several mills that were started up in the 20th century to make vanillin from lignosulphonates soon discontinued production, after it was discovered that vanillin could be made from guaiacol. Today, vanillin is produced from lignosulphonates by Borregaard AS at their Sarpsborg mill in Norway.

Oxidation of the lignin structure produces both aromatic acid and aldehyde products; at severe reaction conditions, the aromatic ring in lignin can open and thereby form organic acids (Ragauskas *et al.* 2014). Many different components form during the oxidation of lignin: in order to reduce their number, it has been suggested that the product fractions of the oxidative treatment be funnelled using microbial metabolic pathways (Abdelaziz *et al.* 2019b).

Another oxidative method that has been investigated is pre-oxidation of the benzylic hydroxyl group present in lignin to form a ketone (Yu *et al.* 2019). This activates the β-O-4' bonds in the lignin, which promotes the use of a milder subsequent depolymerisation strategy less prone to repolymerisation. Oxidation has also been suggested as a way to cleave recalcitrant C-C bonds remaining in lignin when weaker ether bonds have already been cleaved in a previous depolymerisation (Subbotina *et al.* 2021).

2.2.3 Pyrolysis

Heating biomass in the absence of a supply of air causes volatiles to be released from the degraded structure without combustion taking place. These volatiles can then be condensed to form a pyrolysis oil. Non-condensable gases are also formed as well as char (Cao *et al.* 2018). Pyrolysis is a well-researched technique and the biomass is degraded through thermal cracking (Pandey and Kim 2011). A high heating rate favours the production of bio-oil over the formation of char during pyrolysis (Brand *et al.* 2014; Cao *et al.* 2018). Fast pyrolysis therefore is run at approx. 500 °C with heating rates as high as 1000 °C/s (Castello and Rosendahl 2018).

The bio-oil produced by pyrolysis typically has a high oxygen content: around 35 % on a dry basis (Castello and Rosendahl 2018). It also contains a lot of acids and is therefore reactive and repolymerises readily. Moisture is present in the oil, too (Peterson *et al.* 2008). Subjecting it to hydrotreatment, which aims at removing oxygen, is a way of improving the stability of pyrolysis oil. Alternatively, it could be co-processed with fossil oil, e.g. vacuum gas oil (VGO) in a fluid catalytic cracking (co-FCC) process (Castello and Rosendahl 2018).

2.2.4 Hydrothermal treatment

The hydrothermal treatment of lignin encompasses a multitude of treatments that take place in water: the feedstock, lignin or biomass, does therefore not need to be dried in advance as is required for pyrolysis. Using water, a cheap and non-toxic solvent that is readily available, makes these reaction methods attractive (Castello and Rosendahl 2018).

The critical point of water (374 °C, 221 bar) is of the utmost importance in hydrothermal treatments since the properties of water change significantly around this point (Kruse and Dahmen 2015): adjusting either the temperature or the pressure, or both, the properties of water thus can be finetuned. Furthermore, the water functions not only as a solvent but also as a reactant, thereby opening hydrolysis reaction pathways (Cheng *et al.* 2012). Tuning the reaction temperatures thus gives different outcomes, with solid char being the predominant

product at lower temperatures of approx. 200 °C in hydrothermal carbonisation. At higher temperatures of approx. 280-400 °C, liquefaction of the material is possible, whilst at even higher temperatures, i.e. above the critical point, gasification predominates (Kruse and Dahmen 2015; Toor *et al.* 2011). Compared with pyrolysis oil, bio-crude formed via hydrothermal processes typically has a lower oxygen content due to hydrogen donation from the water. This is beneficial to the production of fuel because it reduces the need for subsequent hydrotreatment (Castello and Rosendahl 2018).

A broad classification of hydrothermal treatments is whether they take place in sub or supercritical water. Reaction pathways in subcritical water are typically heterolytic, i.e. ionic, while at supercritical conditions homolytic, i.e. radical, reactions are more prone to occur (Yong and Yukihiko 2013). However, pressure levels in the system also affect the properties of the water: they enable radical reactions to be suppressed by keeping the ionic product high at high pressures despite supercritical temperatures (Castello *et al.* 2018).

Increasing the temperature of water causes the ionic product to increase (Peterson *et al.* 2008). Dissociation of the water molecule thus occurs more easily which, in turn, facilitates ionic reactions taking place in the water. However, at temperatures above 400 °C, the ionic product decreases rapidly and this might partly explain why radical reactions are more prominent at higher temperatures (Lappalainen *et al.* 2020).

The dielectric constant of water also decreases with increasing temperature. Consequently, water behaves more like a non-polar solvent, being able to dissolve non-polar molecules, at high temperature. Indeed, at supercritical conditions, salts may precipitate from the water (Lappalainen *et al.* 2020; Toor *et al.* 2011). Alternatively, depending on the salt and its solubility at higher temperature, a type of brine enriched with salt and a vapour-like salt-depleted fluid of low density may form at supercritical conditions.

During hydrothermal treatment, the products formed are reactive and repolymerisation may therefore occur to varying degrees. This is not unique to hydrothermal treatment: it is also seen in, e.g., pyrolysis and charring in catalytic hydrodeoxygenation (Pandey and Kim 2011; Ragauskas *et al.* 2014). A sequential reaction of depolymerisation, followed by a slower repolymerisation, was suggested by Bobleter and Concin (1979). Repolymerisation causes the formation of char, which may hamper processing in that it blocks tubes and reactor parts and lowers the yield of useful components. Using additions of capping agents to mitigate repolymerisation has been investigated (Dunn and Hobson 2016), based on the idea that the capping agent scavenges reactive components and thus prevents the lignin-derived products from forming char. Along with phenol and boric acids, hydrogen-donating reactants such as formic acid and formate as well as different alcohols have been employed as capping agents (Arturi *et al.* 2017; Belkheiri *et al.* 2018a; Cheng *et al.* 2012; Gosselink *et al.* 2012; Guo *et al.* 2021; Lee *et al.* 2016; Nguyen *et al.* 2014b; Roberts *et al.* 2011; Saisu *et al.* 2003; Toledano *et al.* 2014).

Additions of base to the reaction mixture in the hydrothermal depolymerisation of lignin and biomass have also shown good results in terms of a reduced formation of char and a higher yield of bio-crude (Dunn and Hobson 2016; Toor *et al.* 2011). Such base catalysed

depolymerisation (BCD) has been employed not only in water (Rößiger *et al.* 2018) but also in solvolysis reactions in alcohols (Miller *et al.* 1999; Pandey and Kim 2011).

Besides chemical conditions, temperature and pressure, it can be expected that residence time affects depolymerisation, too. A great deal of research has been undertaken on lignin depolymerisation in batch reactors, where a long residence time is often required to reach the reaction temperature desired compared to a continuous system (Abdelaziz and Hulteberg 2020). As such, studies on systems with short residence times are fairly scarce. A collection of studies pertaining to lignin depolymerisation in both water and alcohols at short residence times are reported, in Table 2. Some highlights are presented below.

Bobleter and Concin worked on depolymerising poplar lignin at short residence times (Bobleter and Concin 1979). Defining a solid residue as being the residue that remained after washing solid products with acetone:water 10:1, they reported that a minimum of solid residue was produced at a residence time of 3 min at 270 °C, and 0.4 min at 365 °C. At longer residence times, the yields of solid residue increased again, and Bobleter and Concin therefore proposed that a rapid depolymerisation was followed by a slower repolymerisation.

Zhang *et al.* investigated the depolymerisation of five different types of lignin at temperatures between 300 and 374 °C without any capping agent (Zhang *et al.* 2008). The heating time of the reactor was 3 min, after which the solid residue after the reaction reached a stable level after 12 min at 300 °C and 3 min at 374 °C: they suggest that initial depolymerisation is fast and is followed by slower repolymerisation. The time scales concur with Cheng *et al.*, who did not report any significant effect on the composition of the product mixture when the residence time in alkaline lignin depolymerisation at 300 °C was varied between 15 and 360 min (Cheng *et al.* 2012). Moreover, Belkheiri, working with kraft lignin depolymerisation in a continuous reactor 350 °C, noted very little effect on the product yields on reducing the residence time from 11 to 6 min (Belkheiri 2018). However, repolymerisation has also been reported to continue with increasing residence time. Wahyudiono *et al.* (2008) investigated the depolymerisation of an alkaline lignin in water without neither a base nor a capping agent added. They reported increasing amounts of solid material, defined as methanol insolubles, being formed on increasing the residence time from 5 to 240 min, including the initial 3 min of heating. This was noted at both 350 and 400 °C, i.e. for sub as well as supercritical systems. Furthermore, it was noted that monomeric compounds such as phenol and cresols increased with residence time. A depolymerisation stage that formed monomers thus occurred simultaneously as a repolymerisation stage to form more solid material.

Work in continuous reactors enables rapid heating and cooling, which may be exploited to investigate shorter residence times (Abdelaziz and Hulteberg 2020). Rößiger *et al.* (2017) depolymerised both organosolv and kraft lignin in a flow reactor with NaOH added. The temperatures investigated ranged between 250 and 340 °C, with estimated residence times in the reactor ranging between 7.5 and 12.5 min. The solid residues, precipitated at pH 1, decreased with increasing temperature and time: this is in contrast to work by Zhang *et al.* (Zhang *et al.* 2008), who reported that the yield of solids first increased and then reached a steady state after 12 min of reaction time at 300 °C. However, Zhang *et al.* did not acidify the reaction product like Rößiger *et al.* did, and Zhang *et al.* also used a batch reactor.

Abdelaziz *et al.* (2018) depolymerised a softwood kraft lignin at temperatures ranging between 170 and 250 °C in a continuous reactor. The molecular weight distribution of the products showed clearly that a mere minute of residence time in the reactor depolymerised the lignin for all temperatures investigated: higher temperatures displayed clearer depolymerisation at this residence time.

Also employing a continuous reactor, Yong and Matsumura (2013) depolymerised lignosulphonates in water at temperatures ranging between 300 and 370 °C with 0.5 to 10 s of residence time. They noted that lignin decomposed within seconds, but also repolymerised and formed char in this brief residence time. Even shorter times were employed by Abad-Fernández *et al.* (2020), who worked with kraft lignin depolymerisation at temperatures between 300 and 400 °C and residence times as short as 60 ms in a continuous set-up. Reactions of the lignin were observed even at this ultrashort residence time. In a follow-up study in the same reactor, Pérez *et al.* (2022) investigated depolymerisation of six different types of lignins: kraft, organosolv and lignin remaining after subcritical water extraction and ultrafast supercritical water hydrolysis of biomass. Working at 386 °C with a residence time at 0.3 s, they concluded that the formation of char was low, since they reduced repolymerisation by employing a low residence time. Lastly, when depolymerising sulphonated kraft lignin at 385 °C for 370 ms, Adamovic *et al.* (2022) noted the formation of diphenylmethanes in the solid residue after reaction, as evidenced by nuclear magnetic resonance (NMR) spectra of the solid residue. They argued that formation of these species contributes to repolymerisation, even though this residence time was too short for all the inter-unit ether linkages in the lignin to be broken.

These studies, along with the others presented in Table 2, suggest that lignin depolymerisation under hydrothermal treatment can be a rapid process. The combination of the addition of a capping agent such as an alcohol and short residence times has been researched to a lesser extent, and especially so in the case of kraft lignins. The work undertaken to explore these effects is presented in the chapters that follow.

Table 2: Compilation of studies on hydrothermal lignin depolymerisation with short residence times. Softwood (SW); hardwood (HW).

Study	Lignin	Lignin conc. [wt%]	Reactor	T [°C]	Residence time [s]	Residence time [min]	Solvent	Pressure [MPa]	Co-solvent/ capping agent	Catalyst	Method used to track depolymerisation
(Bobleter and Concin 1979)	HCl hydrolysis lignin (HW)	2	Batch, 8 ml	270–372	24–900 (incl. heating)	0.4–15 (incl. heating)	Water	Not stated	--	--	Yield of solid residue after 10:1 acetone:water extraction
(Miller *et al.* 1999)	Organosolv (HW) and Indulin AT (kraft SW)	Approx. 10	Batch, 14 ml	290	0–3600 (+90 s heating and 30 s additional cooling)	0–60 min (+1.5 min heating and 0.5 min quenching)	EtOH or MeOH	Not stated	--	KOH, NaOH, CsOH, LiOH, $Ca(OH)_2$, and Na_2CO_3	Yield of precipitates at pH 2 washed with water and DEE
(Saisu *et al.* 2003)	Organosolv lignin	1.5–2	Batch, 10 ml	400	300–3600 (of which 240 s heating + 60 s additional cooling)	5–60 (of which 4 min heating + 1 min additional cooling)	Water	Not stated	Phenol	--	Yield of THF insolubles and THF solubles
(Okuda *et al.* 2004)	Organosolv lignin	2.2–3.8	Batch, 5 ml	400	360–3600 (+240 s heating)	6–60 (+4 min heating)	Water	Estimated at <37	Phenol	--	GPC profile of whole reaction mixture
(Wahyudiono *et al.* 2008)	Alkaline lignin	3–11	Batch, 5 ml	350–400	300–14400 (of which 180 s heating)	5–240 (of which 3 min heating)	Water	25–40	--	--	Yield of MeOH-insolubles (MI)
(Zhang *et al.* 2008)	2 kraft lignins (SW), organosolv lignin from oat hull, 2 acid hydrolysis lignin (HW and switchgrass)	10	Batch, 75 ml (induction heating)	300–374	60–1800 (+150-180 s heating and 300 s cooling)	1–30 (+2.5-3 min heating and 5 min cooling)	Water	10–22	--	--	Yield of solid residue after acetone extraction
(Roberts *et al.* 2011)	Organosolv lignin	2.5-10	Continuous	240–340	120–900	2–15	Water	25-31.5	--	NaOH	Oil yield (EtOAc extract)
(Roberts *et al.* 2011)	Organosolv lignin	2.5	Batch, 5.6 ml	270–360	1200–3600	20–60	Water	Not stated	Boric acid	NaOH	Oil yield (EtOAc extract)
(Cheng *et al.* 2012)	Alkaline lignin	9–11	Batch, 14 ml and 75 ml	200–450	900–21600 (+60–120 s heating)	15–360 (+1–2 min heating)	Water/ EtOH	5 at the beginning, increasing when heated	$H_{2(g)}$	$Ni10/Al_2O_3$, $Ru10/Al_2O_3$, Pt10/AC	Yield of solid residue, degraded lignin and water-soluble product
(Yong and Matsumura 2012)	Alkaline lignosulphonates (SW)	0.1	Continuous, 1 mm diameter	390–450	0.5–10	0–0.17	Water	25	--	--	Yield of residual lignin
(Yong and Matsumura 2013)	Alkaline lignosulphonates (SW)	0.1	Continuous, 1 mm diameter	300–370	0.5–10	0–0.17	Water	25	--	--	Yield of residual lignin
(Rößiger *et al.* 2017)	Organosolv lignin (HW), kraft lignin (SW)	Organosolv, 2.5–10; Kraft, 2.5–7.5	Continuous, 2.7 l	240–340	450–900	7.5–15	Water	25	--	NaOH	Oil yield (MIBK extract) and precipitated oligomers
(Abdelaziz *et al.* 2018)	Kraft lignin (SW)	5	Continuous, 18 ml heated, 50 ml total	170–250	60–240	1–4	Water	12–13	--	NaOH	GPC profile

Study	Lignin	Lignin conc. [wt%]	Reactor	T [°C]	Residence time [s]	Residence time [min]	Solvent	Pressure [MPa]	Co-solvent/ capping agent	Catalyst	Method used to track depolymerisation
(Belkheiri 2018)	Kraft lignin (SW)	5.5	Continuous, 500 ml	350	360–660	6–11	Water	25	Phenol	KOH+ K_2CO_3, ZrO_2	Yield of solid residue, bio-oil; yield of water-soluble organics.
(Otromke *et al.* 2019b)	Kraft lignin (SW) extracted with MeOH	Approx. 10	Continuous, 50 ml	300	480–1440	8–24	Water	18	--	NaOH	GPC profile and NMR spectra
(Abad-Fernández *et al.* 2020)	Kraft lignin	0.1	Continuous, 0.5-12.3 ml	300–400	0.06–4.6	0–0.08	Water	26	--	--	Oil yield (EtOAc extract)
(Pérez *et al.* 2022)	Sulphonated kraft (SW), kraft (HW), organosolv (HW), kraft black liquor (HW), sub and supercritical extracted wheat straw, beet pulp & tobacco	0.5	Continuous, 1.6 ml	386	0.30	0.005	Water	260	--	NaOH	GPC profiles; yields of oil and monomer
(Adamovic *et al.* 2022)	Sulphonated kraft lignin and kraft lignin	0.5	Continuous	385	0.37	0.006	Water	254	Vanillyl alcohol, vanillin, vanillic acid, acetovanillone	NaOH	Consumption of model compounds added; yields of solid residue, oil, HSQC and GPC

3
Methods and Materials

This chapter begins with a recount of the reactor and its operation during lignin depolymerisation, the fractionation and characterisation of the product and a description of the analytical methods employed in this work; exact details of the operation are provided in the appended papers. The test plans, along with motivations for the operating conditions chosen, follow, together with an overview of the experiments performed in the reactor. Finally, the lignin and chemicals used are described.

3.1 Hydrothermal treatment

The softwood kraft lignin was depolymerised at 250 bar in a batch reactor 99 ml in size, the wetted parts of which are made out of Inconel 625. The whole set-up is manufactured by SITEC-Sieber Engineering AG (Zürich, Switzerland) and is equipped with two hand pumps for injection of material at high pressure, one of which was used in this work, see Figure 4. A more in-depth description of the reactor is provided by Arturi *et al.* (2017).

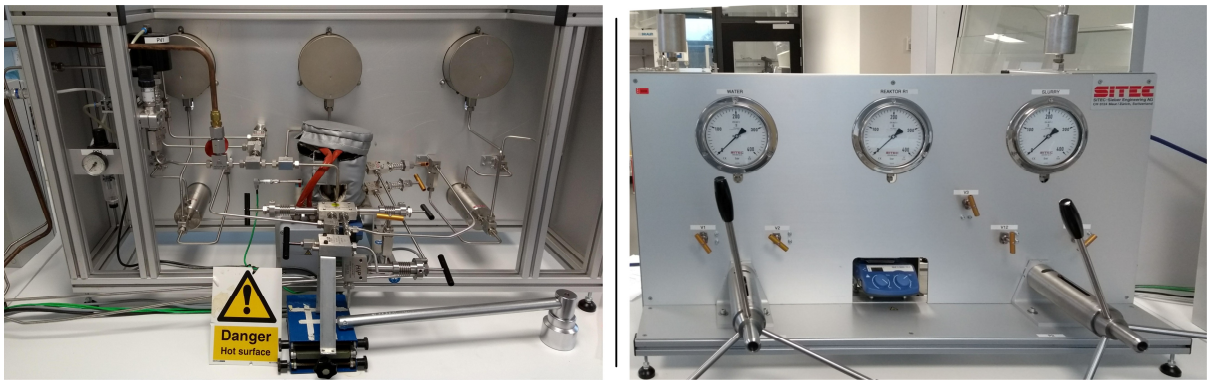

Figure 4: Rear and front images of the reactor used. Left: reaction vessel. Right: hand pumps and pressure meters.

3.1.1 Preparation of the reaction charge

The reaction charge was split into two parts: a pre-charge (constituting 57 wt% ± 4 wt% of the total reaction mixture) containing water and bases (Na_2CO_3 and NaOH), and an injection charge (43 wt% ± 4 wt% of the total reaction mixture) containing water, bases (Na_2CO_3 and NaOH), capping agent (isopropanol, glycerol or guaiacol) and lignin. This allowed the reactive components to be injected into the pre-heated, non-reacting, pre-charge and rapid heating of the reactants could thus be achieved.

With the addition of isopropanol, using only Na_2CO_3 as the base, the dissolution of lignin in the reaction medium was smooth, see Papers I and II. The solution was mixed and left to dissolve overnight, which yielded a satisfactory dissolution except when the isopropanol addition (0-24 wt% of the reaction charge) was at its lowest levels. In those cases, the mixture was dispersed using an Ultra Turrax® (IKT T25; IKA-Werke GmbH & Co. KG., Staufen, Germany) at 20 000 rpm for 15-30 min to properly disperse the lignin. With the addition of glycerol (15-17 wt% of the reaction charge) and guaiacol (0.2-2.2 wt% of the reaction charge) however, see Papers III and IV, it was more challenging to dissolve the lignin so NaOH was added to raise the pH and improve its dissolution. These mixtures were also dispersed using the Ultra Turrax® at 15 000 rpm for 15 min. The mixtures were all prepared immediately prior to injection because the undissolved lignin settled when left overnight.

3.1.2 Reactor operation

A P&I diagram of the reactor is presented in Figure 5. The pre-charge was added to the reactor (R1 in Figure 5) and a stream of N_2 was used to displace air before it was sealed. The pre-charge was then heated to 25 °C ± 7 °C above the target reaction temperature, thus forming a mixture of vapour and liquid. The injection charge was pumped into this mixture of vapour and liquid by the hand pump (P2) shown in Figure 5. At the time of injection, the pressure inside the reactor was close to the vapour pressure of water at the current temperature. As the injection charge was being pumped into the reactor, the pressure rose rapidly as the whole reactor was filled with reaction liquid. An injection took, on average, 47 s ± 17 s, with the ensuing temperature drop being recovered within 1 min 33 s ± 47 s. The lignin and capping agent were thus heated quickly to the reaction temperature, partly by heat from the condensing vapour. The pressure continued to rise as the temperature rose. Since the reaction mixture remained a liquid, the pressure could be fine-tuned by making small injections and removing reaction mixture, <1ml, with the hand pump (P2 in Figure 5).

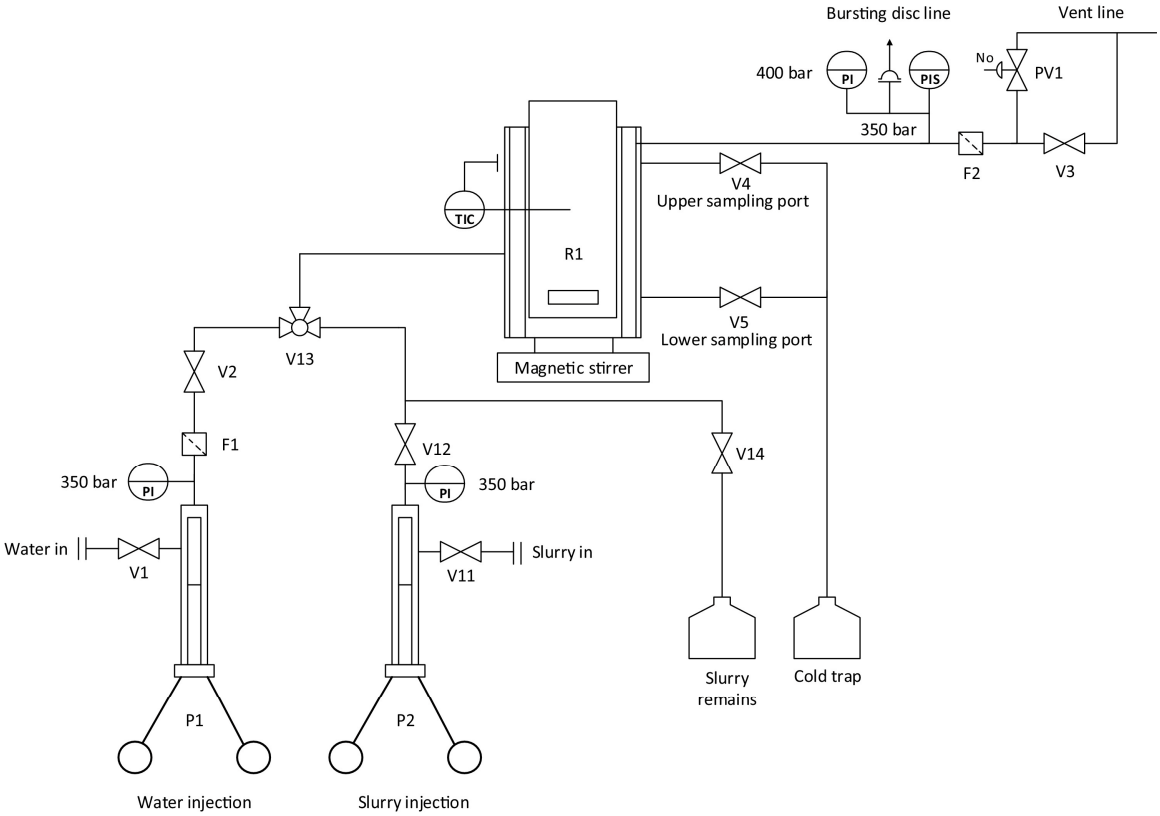

Figure 5: Schematic diagram of the reactor set-up.[1] The water injection pump (P1) was not used in this work.

The residence time in the reactor was defined as the time from the end of the injection to the start of the discharge. At the beginning of the residence time, the reactor was at its coldest because the injection charge was at room-temperature. Consequently, the reactor temperature and pressure, which were measured every tenth second, rose as the reactions progressed. Average temperatures and pressures were therefore calculated according to:

$$y_{avg} = \int_{t_1}^{t_2} \frac{y(t)}{t_2 - t_1} dt \quad (1)$$

where y_{avg} was the average temperature or pressure, t_1 the time after injection, t_2 the time at discharge and $y(t)$ the temperature or pressure at time t. Pressure and temperature profiles in the reactor are provided in *Appendix I - Reaction temperature and pressure profiles.*

Once the prescribed residence time had elapsed, the reaction mixture was discharged, through valve V5 in Figure 5, into a cold trap consisting of 200 g water in a flask equipped with a condenser set in an ice-bath. The reaction was thus quenched quickly in the cold water and the reaction mixture was diluted.

3.1.3 Fractionation of the reactor product

The reactor product, which was comprised of the reaction mixture and the water from the cold trap, was fractioned according to Figure 6, with some minor adaptations for each study. The

[1] Reprinted from Arturi, K.R., Strandgaard, M., Nielsen, R.P., Søgaard, E.G. and Maschietti, M. (2017). Hydrothermal liquefaction of lignin in near-critical water in a new batch reactor: Influence of phenol and temperature. *J. Supercrit. Fluids* 123: 28–39, with permission from Elsevier.

reaction mixture was first filtered over glass filters (#5, nominal cut-off: 1.0-1.6 µm) and, in the case of guaiacol addition, the filter cake was washed with water to remove residual guaiacol, Paper IV. The filter cake was dried for four days in 40 °C and subsequently denoted *char*. The temperature was deliberately set low to avoid reactions occurring in the char during drying.

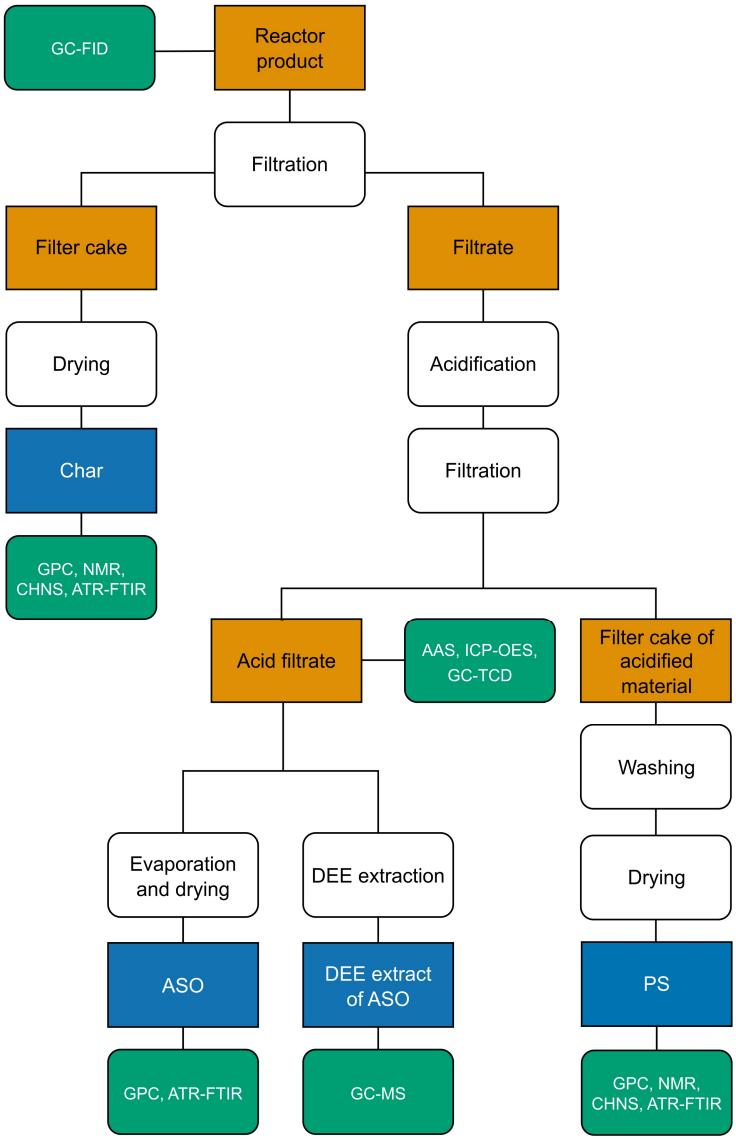

Figure 6: Fractionation of the reactor product into the different product fractions (blue) and ensuing characterisations (green).

The filtrate was a brown opaque liquid that was acidified with 1 M HCl, using an auto-titrator (Titro-Line 7000, SI Analytics; Xylem Analytics Germany GmbH, Welheim, Germany), to pH 1.5, which caused the precipitation of a brown material as well as the release of CO_2 from the residual carbonates from the added Na_2CO_3. The acidified filtrate was again filtered (#5, nominal cut-off: 1.0-1.6 µm) and washed with a ratio of 1:1 w/w amount of water to acidified filtrate. The filter cake was then dried for five days in 40 °C after which it was denoted precipitated solids, *PS*.

The water in the acidified filtrate was evaporated in ambient conditions for three days, followed by one day in 40 °C. A resulting mixture of salt crystals and organic material was thus formed.

Glycerol, when added to the reaction mixture, remained in this fraction: the content remained fluid, even upon prolonged drying at elevated temperatures. Consequently, the glycerol content was estimated using gas chromatography, which is described below. When isopropanol and guaiacol were used, on the other hand, the resulting residue after evaporation was solid: no residual capping agent was present. The salt content of the acidified filtrate was estimated by measuring the sodium content using either atomic absorption spectroscopy (AAS) or inductively-coupled plasma–optical emission spectrometry (ICP-OES). Based on the assumption that all of the sodium formed NaCl (from the neutralisation of NaOH and Na_2CO_3 with HCl), the salt content was then deducted from the weight of the residue, thereby allowing the content of acid soluble organics, *ASO*, to be quantified.

The yields of the product fractions were defined on a dry lignin basis thus:

$$Y_i(\%) = 100 * \frac{m_i}{m_{dry\ lignin}} \quad (2)$$

where Y_i is the yield of component i, m_i is the mass of component i and $m_{dry\ lignin}$ is the amount of dry lignin loaded into the reactor. In the case of ASO, salt was deducted; when glycerol was used as the capping agent, the estimated content of glycerol was deducted from the yield of ASO.

3.2 Characterisation of the products

The analyses made of the product fractions are outlined in the following section. Details pertaining to the set-up in the specific studies can be found in the appended papers.

3.2.1 Residual capping agents and salts

Residual capping agents in the reaction mixture were quantified using gas chromatography equipped with a flame ionisation detector and a thermal conductivity detector (GC-FID and GC-TCD). Salts in the acidified reaction mixture that were formed through neutralisation of the NaOH and Na_2CO_3 by HCl were identified by measuring the content of sodium in the acidified filtrate using AAS and ICP-OES.

3.2.1.1 GC-FID

The residual content of guaiacol in the product mixture after reaction was measured using gas chromatography with a flame ionisation detector (PerkinElmer Clarus 690; PerkinElmer inc., Waltham, Massachusetts, USA). 1 ml product phase was acidified with 0.3 ml 2 M HCl to pH 0-1 and 1 ml of the acidified product phase was mixed 1:1 v/v with internal standard solution (4 g/l phenol in water), before being filtered with a 0.45 µm syringe filter and run in GC-FID. Phenol was used as an internal standard even though it was formed during the reaction: this was possible because the amount of phenol formed was very low, being <0.1 wt% of the amount of phenol added, see Paper IV. The column employed was an Elite BAC-1 Advantage; information on the temperature programme used is provided in Paper IV. Duplicate samples were run, with double injections, and the average relative standard deviation (RSD) was 2.5 %.

3.2.1.2 GC-TCD

The glycerol that remained in the acid filtrate, and subsequently ended up in the ASO fraction, was quantified using gas chromatography with a thermal conductivity detector (GC-TCD; Agilent 7890A; Agilent Technologies Co. Ltd., Shanghai, China and G3437A; Agilent

Technologies Co. Ltd., Shanghai, China). The acid filtrate was diluted 1:10 with water and to this was added an internal standard solution with cyclohexanol. The content of cyclohexanol was 2.05 g/l in the samples, and they were filtered with a 0.45 µm filter. Samples were run through an HP-5MS UI column (Agilent Technologies Inc., Santa Clara, CA, USA), with helium as the carrier gas; information on the temperature programme employed is given in Paper III. Duplicate samples were run, and the average RSD was 2.1 %.

3.2.1.3 AAS and ICP-OES

In Paper I, the sodium content was measured using AAS with a hollow cathode Na-lamp at 330.3 nm (Thermo Scientific iCE3000; Thermo Fisher Scientific, Cambridge, UK). The acid filtrate was diluted 1:10, filtered with a 0.45 µm syringe filter and run in the AAS. SOLAAR (v. 11.02) was used for data processing and samples were run in triplicate, with an average RSD of 0.89 %.

In Papers II-IV, the sodium content was measured using inductively-coupled plasma–optical emission spectrometry (Thermo Scientific iCAP Pro, Thermo Fischer, Cambridge, UK). The acid filtrate was filtered once again, using a 0.45 µm syringe filter. Then, samples were diluted 1:20 (Paper II) and 1:50 (Papers III and IV) with 0.5 M HNO_3 and an internal standard of 2 ppm yttrium was added. The emission lines at 818 nm (Paper II) and 589.59 nm (Papers III-IV) for sodium were measured in triplicate, with an average RSD of 6.4 %.

3.2.2 Melting points, moisture content and elemental analyses

The moisture content of the kraft lignin was measured using a moisture analyser operating at 105 °C (Sartorius, MA30; Sartorius, Göttingen, Germany).

The elemental compositions of the lignin, char and PS fractions were determined by CHNS combustion analysis in pure oxygen, using helium as the carrier gas (Elementar vario MICRO Cube, Elementar Analysensysteme GmbH, Langenselbold, Germany). Samples were pre-dried overnight at 105 °C to dispel moisture. 2 mg of lignin, char and PS, respectively, were added to tin weighing boats and loaded in the MICRO cube. The contents of carbon, hydrogen, nitrogen and sulphur were determined with combustion and reduction temperatures of 1150 and 850 °C, respectively, whilst the oxygen content was calculated by difference. Duplicate samples were run; the RSD was 0.46 % for C, 0.54 % for H, 10.8 % for S and 1.6 % for O. Sulphanilamide was used for calibration.

The melting points of the products obtained were investigated by heating the samples at a rate of 20 °C/min from ambient temperature up to 375 °C on a heating plate (Mettler FP82HT Hotstage and Mettler FP90, Mettler-Toledo GmbH, Greifensee, Switzerland) whilst observing them with a light microscope (Olympus BH-2, Olympus Corporation, Tokyo, Japan).

3.2.3 Molecular weights

Gel permeation chromatography (GPC; PL-GPC 50 Plus Integrated GPC system, Polymer Laboratories; Varian Inc., Church Stretton, UK) was used to determine the molecular weight distributions of the lignin and product fractions, employing two PolarGel-M columns (300×7.5 mm) and a pre-column (PolarGel-M, 50×7.5 mm). The system was equipped with an ultraviolet light (UV) detector operating at 280 nm and a refractive index (RI) detector. Subsequent calculations of M_w were made using Cirrus GPC Software (v. 3.2).

Samples were dissolved overnight in dimethyl sulphoxide (DMSO) with 10 mM LiBr. The samples, which were dark and opaque, were then diluted to a concentration of 0.24 mg/ml and filtered through 0.2 µm syringe filters. Although no solids were apparent at the time of dilution of the dissolved material, prolonged storage nevertheless showed an unquantified settling of solids in the non-diluted samples. In the diluted samples run in the GPC, however, no solids were noted. In some cases, concentrations of 1.5 and 3 mg/ml were used for the ASO samples, see Papers III and IV, to obtain a sufficiently strong signal since a 0.24 mg/ml dilution gave too weak signals. The eluent flow rate was set at 0.5 ml/min and the temperature at 50 °C.

Calibration was made using pullulan standards (PL2090-0100 [180 - 708 000 Da], Varian, Church Stretton, UK) using an RI detector. Lignin and pullulan, however, have different hydrodynamical volumes which introduce an error in the measurements of molecular weights. However, polystyrene standards, which resemble lignin more closely than pullulan, are not readily solvable in DMSO (Sulaeva *et al.* 2017). Comparisons between the samples, rather than their absolute molecular weights, are therefore emphasised in this thesis (Zinovyev *et al.* 2018). The average RSD from duplicate injections was 0.58 %.

3.2.4 Molecular structure and functional groups

Investigations into the molecular structure of the lignin and products, as well as functional groups, were undertaken using NMR spectroscopy and attenuated total reflection–Fourier transform infrared spectroscopy (ATR-FTIR).

3.2.4.1 NMR

Investigations of the molecular structure of the lignin, char and PS were made using NMR employing the ^{1}H-^{13}C heteronuclear single quantum coherence (HSQC, *hsqcedetgpsisp2.3*), heteronuclear multiple bond correlation (HMBC, *hmbcetgpl3nd*) and ^{1}H (*zg30*) pulse sequences, all recorded at 25 °C. The HSQC were recorded in edited mode, so that CH and CH_3 correlations are positive and CH_2 are negative.

NMR analysis using HSQC shows the single bond correlations between carbon and hydrogen atoms. Therefore it cannot be employed directly to investigate carbonyl carbons, aside from aldehydes: carbonyl carbon does not have a direct connection to a hydrogen atom, so there is no C-H bond correlation to detect. The HMBC, in which multiple bond correlations of carbon and hydrogen are found (McClelland *et al.* 2017), was therefore used as a complement to HSQC.

Samples were dissolved to a concentration of 140 mg/ml in deuterated DMSO-*d6* in Eppendorf tubes before being centrifuged at 12045-20879×g for 5 min; the supernatant was then transferred to 3 mm tubes. In a number of instances, the samples contained some non-dissolved materials: these were not analysed by NMR (Papers I-III). This non-dissolved fraction, which typically occurred in char samples, was estimated as being <5 wt% of the samples and thus not anticipated to affect the main conclusions of this work.

Two spectrometers were used for both HSQC and HMBC: a 700 MHz spectrometer equipped with a 5 mm QCl cold probe (Bruker Avance III; Bruker BioSpin GmbH, Rheinstetten, Germany) and an 800 MHz spectrometer equipped with a 5 mm TXO cold probe (Bruker

Avance III HD; Bruker BioSpin GmbH, Rheinstetten, Germany). Details pertaining to the set-up of the pulse sequences can be found in the appended papers.

Data processing was carried out using MestReNova (v. 10.0.2) with a polynomial baseline correction of order 3. Phase correction was made starting with an automatic phase correction, followed by minimising the PH1 correction to 0 in both dimensions, and then manual phasing after the methoxy peak. The central solvent peak, DMSO-*d6* at 2.50 and 40.2 ppm, was used for chemical shift calibration.

3.2.4.2 ATR-FTIR

Attenuated total reflection–Fourier transform infrared spectroscopy (PerkinElmer Frontier FT-IR, PerkinElmer Inc. Waltham, Ma, USA and GladiATR-FTIR, PIKE Technologies, Madison, WI, USA) was used to investigate the functional groups of the lignin and product fractions. Spectra were recorded between 4000 and 400 cm^{-1} with 10 scans per sample and a 4 cm^{-1} resolution. The ASO fractions, which were not dried at 40 °C for as long as the char and PS, were freeze-dried before ATR-FTIR measurement (FreeZone Triad 7400030 freeze drier, Labconco Corporation, Kansas City, MO, USA). Spectral processing was carried out using PerkinElmer Spectrum (v. 10.4.3) and MATLAB R2020b.

3.2.5 Identification of monomers

Identification and semi-quantification of the monomeric products formed during the reactions were performed using gas chromatography – mass spectrometry (GC-MS).

3.2.5.1 GC-MS

Samples of the monomeric products were prepared for GC-MS analysis by taking 5 ml or 10 ml acidified filtrate and adding 0.5 ml or 1 ml internal standard solution (1 g/l syringol in water), respectively, and then extracting the mixture with diethyl ether (DEE), 1:1 *w/w*. Syringol was chosen as the internal standard since it is similar to the products anticipated. Moreover, it is presumed that syringol is not formed to any large extent since the lignin was sourced from softwood, which lacks syringyl units (Nguyen *et al.* 2014b). In Paper I, the extracted acidified material was merely settled and not filtered: in Paper II, it was centrifuged and not filtered, but this is not expected to affect the results.

The ether phase was filtered with a 0.45 µm filter and run in GC-MS (Agilent 7890A, Agilent Technologies Co. Ltd., Shanghai, China and Agilent 5975C, Agilent Technologies Inc., Wilmington, DE, USA). The column was an HP-5MS UI column (Agilent Technologies Inc., Santa Clara, CA, USA) and helium was used as the carrier gas. Details of the temperature programme are provided in the appended papers.

Identification of the products was carried out using the software Enhanced ChemStation (E.02.02.1431) and NIST MS Search (v. 2.2) employing the Mass Spectral library NIST11. Furthermore, this was confirmed by matching the retention times of pure components with those of the components in the sample. Semi-quantification of the monomers identified was made according to (Nguyen *et al.* 2014b) using the following expression:

$$W_i = W_{IST} \frac{A_i}{A_{IST}} \quad \textbf{(3)}$$

where W_i and W_{IST} are the mass fractions of component *i* and the internal standard *IST* in the sample, respectively. A_i and A_{IST} are the peak areas in the chromatogram for component *i* and the internal standard *IST,* respectively. The average RSD based on duplicate and triplicate runs was 5.5 %.

3.3 Test plan

The softwood kraft lignin used in this work was separated from black liquor by the LignoBoost process. It was depolymerised in alkaline water in subcritical water, with an initial residence time of 12 min being set, which is in accordance with similar work by Arturi *et al.* and Nguyen *et al.* (Arturi *et al.* 2017; Nguyen *et al.* 2014b). Nguyen *et al.* had worked on the same LignoBoost lignin as used in this work (Nguyen *et al.* 2014b), and Arturi *et al.* had used the same reactor (Arturi *et al.* 2017). Shorter residence times, 1-12 min, were also investigated.

The temperature range investigated was 290-335 °C, although the highest temperature was initially envisioned as being at 350 °C, like in the work of Nguyen *et al.* (Nguyen *et al.* 2014b). However, isopropanol has been observed to decompose at temperatures above 335 °C, so this was set as a highest temperature (Ross and Blessing 1979). An intermediate temperature level of 320 °C was chosen because Arturi *et al.* noted the highest yield of aromatic monomers at this temperature (Arturi *et al.* 2017). Finally, 290 °C was set somewhat arbitrarily as a lower reaction temperature; it was employed for investigations into the effect of the residence times, namely 1-12 min. The reactor runs in this work are compiled in Table 3, according to their respective paper. Average temperatures and pressures T_{avg} and P_{avg} are calculated using the expression **(1)**. Notably, average temperatures and pressures differed from the set points since the reaction mixture was heated after injection.

The ratio between capping agent and kraft lignin was investigated with the intention of running the reactor ratios 0, 0.5, 2 and 5 by weight (capping agent over lignin). In order to maintain the pressure levels, more injection charge than was anticipated had to be injected, making the final ratios 0, 0.6, 2.7 and 4.9, which corresponds to 0, 4, 13 and 24 wt% isopropanol in the reaction feed. When investigating the reaction temperature and residence time, a mass fraction of 13 wt% isopropanol in the feed was chosen as being sufficient; the addition of this level of isopropanol dispersed favourably, or even dissolved, the lignin and thereby facilitated treatment.

The same level of capping agent in the feed was used for glycerol (15-17 wt%), although the lignin did not dissolve as satisfactorily. In the case of guaiacol, on the other hand, the greatest amount used in the reaction mixture was 2.2 wt%, which corresponds to a guaiacol mass fraction in the injection charge of around 5 wt%: at higher levels, a viscous guaiacol-rich phase separated out. Moreover, Belkheiri *et al.* did not see any improvement in the yield of bio-oil or water soluble monomers when they used more than 2 wt% phenol in the reaction feed (Belkheiri *et al.* 2018a), so the highest intended level of guaiacol was therefore 2 wt%, which after maintaining reactor pressure became 2.2 wt%. The guaiacol series also included a test run with 0.2 wt% guaiacol in the reaction mixture. Work in the preceding studies (Papers I-III) had shown that the amount of guaiacol produced from the lignin, which is the most prevalent monomer, was around this level. Hence, it was chosen as a level of addition to

examine whether it had any effect on the process; if it did, then recirculation of product material could be envisioned.

In the first two studies (Papers I and II), the only salt added was sodium carbonate. However, in the later studies, the lignin did not dissolve properly in the injection charge and, as a consequence, it was difficult to pump the mixture. This problem was mitigated by adding NaOH to raise the pH and thus improve the solubility of the lignin.

Table 3: Residence time, average temperature and pressure, composition of the feed solution and the pH of the reaction product after dilution in the cold trap for the reactor runs. Bold entries highlight the parameter investigated. N.B. In the first paper, the sample run at T_{avg} = 321 °C and 12.9 wt% isopropanol in the feed was used in both the temperature and isopropanol series.

Capping agent	Residence time [min]	T_{avg} [°C]	P_{avg} [bar]	pH of reaction product	NaOH [wt%]	Na_2CO_3 [wt%]	Water [wt%]	Capping agent [wt%]	Lignin (dry) [wt%]
Paper I									
Isopropanol	12	313	250	8.7	--	1.6	92.9	**0.0**	5.5
	12	314	248	8.7	--	1.6	88.9	**3.6**	5.9
	12	321	247	9.2	--	1.6	80.7	**12.9**	4.8
	12	314	243	9.0	--	1.6	69.3	**24.2**	4.9
	12	319	242	9.2	--	1.6	85.0	**13.4**	0.0
	12	**293**	256	8.9	--	1.6	78.0	14.9	5.5
	12	**321**	247	9.2	--	1.6	80.7	12.9	4.8
	12	**334**	248	9.2	--	1.6	80.6	13.0	4.8
Paper II									
Isopropanol	**1**	276	227	9.6	--	2.1	79.4	13.5	5.0
	2	284	247	9.3	--	2.1	81.4	12.0	4.5
	4	289	247	9.3	--	1.6	80.6	13.0	4.8
	12	292	246	9.7	--	2.1	80.5	12.7	4.7

Capping agent	Residence time [min]	T_{avg} [°C]	P_{avg} [bar]	pH of reaction product	NaOH [wt%]	Na_2CO_3 [wt%]	Water [wt%]	Capping agent [wt%]	Lignin (dry) [wt%]
Paper III									
Glycerol	**1**	281	227	10.7	1.0	1.6	75.7	15.9	5.8
	1	270	229	10.5	1.0	1.6	74.7	16.5	6.1
	2	272	251	10.7	1.0	1.6	75.0	16.3	6.0
	4	285	249	10.4	1.0	1.6	75.9	15.7	5.8
	4	281	250	10.4	1.0	1.6	76.7	15.1	5.6
	12*	291	258	9.9	1.0	1.6	74.0-76.3*	15.5-17.2*	5.7-6.3*
	4	281	251	9.3	0.0	1.6	76.6	15.9	5.9
	4	290	247	10.7	1.0	1.6	92.3	0.0	5.1

*The amount of injection charge at 12 min was uncertain, so ranges of the glycerol, lignin and water injected are therefore given.

Paper IV									
Guaiacol	**4**	294	243	12.4	1.0	1.6	95.2	**2.2**	0.0
	1	291	214	10.9	1.0	1.6	92.2	**0.0**	5.2
	1	291	249	10.3	1.0	1.6	90.0	**2.1**	5.3
	4	288	247	10.5	1.0	1.6	91.9	**0.0**	5.5
	4	294	214	10.1	1.0	1.6	92.1	**0.0**	5.3
	4	293	248	10.5	1.0	1.6	92.1	**0.2**	5.1
	4	295	249	10.1	1.0	1.6	91.0	**1.1**	5.3
	4	301	251	10.0	1.0	1.6	89.9	**2.2**	5.4
	4	296	241	10.2	1.0	1.6	90.2	**2.1**	5.2
	12	295	248	10.1	1.0	1.6	89.8	**2.2**	5.4

3.4 Materials

The lignin used was extracted from a softwood black liquor (from a mixture of *Pinus sylvestris* and *Picea abies)* using the LignoBoost process at the Bäckhammar mill in Sweden. The same batch of lignin was used in all of the studies made. It had a dryness of 80.5 wt% ± 3.1 wt% (Sartorius MA30 moisture analyser; Sartorius, Göttingen, Germany) and an M_w of 12.3 kDa ± 0.7 kDa. This is the average value of the LignoBoost lignin M_w for all the measurements made in the appended papers. In the subsequent presentations of each study, the lignin M_w measured is presented for each particular study and it differs somewhat from the average. The elemental composition of the lignin is given in Table 4. The ash content of the lignin has been reported previously as being 0.8 wt% (Nguyen *et al.* 2014b).

Table 4: Elemental composition of the initial softwood LignoBoost lignin, based on measurements made in duplicate, with the corresponding standard deviation. N.B. The standard deviation for carbon and hydrogen is very low.

Element	Composition [wt%]
C	68.0 ± 0.0
H	5.7 ± 0.0
O[a]	24.4 ± 0.1
S	1.97 ± 0.2

[a] Calculated by difference.

The softwood kraft lignin was depolymerised in a mixture of **deionised water**, **anhydrous Na_2CO_3** (≥99.9 %, VWR Chemicals, Leuven, Belgium; and Merck, Darmstadt, Germany; and >99.5 % J.T. Baker, Deventer, The Netherlands) and capping agent: **isopropanol** (≥ 99.9 %, VWR Chemicals, Fontenay-sous-Bois, France), **glycerol** (≥ 99.9 %, VWR Chemicals, Leuven, Belgium) or **guaiacol** (≥ 99 %, Sigma-Aldrich, Steinheim, Germany). When glycerol and guaiacol were used, **NaOH** (≥99 %, Merck, Darmstadt, Germany) was also added to the reaction mixture. For the separation and analysis, the following were all used as received: **HCl** (1 M, Honeywell Fluka, Seelze, Germany), **NaCl** (≥99.5 %, Merck, Darmstadt, Germany), **LiBr** (>99 %, Sigma-Aldrich, Steinheim, Germany), **pullulan standards** (PL2090-0100, Varian, Church Stretton, UK), **dimethyl sulphoxide** (DMSO, >99.7 %, Sigma-Aldrich, Steinheim, Germany), **nitric acid** (65 %, Merck Suprapur, Darmstadt, Germany), **sodium standard** (UltraScientific, North Kingstown, USA), **diethyl ether** (DEE, >99.0 % with >1 ppm BHT as inhibitor, Sigma-Aldrich, Steinheim, Germany; and ≥99.7 % stabilised with BHT, VWR Chemicals, Leuven, Belgium), **cyclohexanol** (99 %, Sigma-Aldrich, Steinheim, Germany), **vanillin** (99 % Sigma-Aldrich, Steinheim, Germany), **guaiacol** (Sigma-Aldrich, Steinheim, Germany), **syringol** (99 %, Sigma-Aldrich, Steinheim, Germany), **1,2-dihydroxybenzene** (>99 %, Sigma-Aldrich, Steinheim, Germany), **acetovanillone** (≥98 %, Sigma-Aldrich, Steinheim, Germany), **4-methylguaiacol** (≥98 %, Sigma-Aldrich, Steinheim, Germany), **homovanillic acid** (Sigma-Aldrich, Steinheim, Germany), **4-ethylguaiacol** (≥98 %, Sigma-Aldrich, Steinheim, Germany), **1,2-dimethoxybenzene** (99 %, Sigma-Aldrich, Steinheim, Germany), **DMSO-*d6*** (99.5 atom % D, 0.03 (v/v) TMS, Sigma-Aldrich, Steinheim, Germany) and **sulphanilamide** (≥ 99 %, Elementar Analysensysteme, Langenselbold, Germany). 1 M **HCl** (37 %, Sharlau, Sentmenat, Spain) was also diluted in-house.

4

Results and Discussion

Results of the investigations of the lignin depolymerisation are presented in three sections, beginning with general findings of the hydrothermal treatment. The effect of residence time is then discussed, along with notes on the impact of temperature and, finally, the effects of using isopropanol, glycerol and guaiacol as capping agents are presented.

4.1 Hydrothermal treatment of softwood kraft lignin

The hydrothermal depolymerisation of softwood kraft lignin performed at 250 bar, 290-335 °C and 1-12 min, and ensuing quenching in ice-cold water, produced an aqueous suspension that was dark in colour and had a strong, smoky odour. No separate liquid organic phase was produced at the conditions investigated, regardless of the capping agent added. This concurs with similar lignin depolymerisation work employing water mixtures with: methanol (Belkheiri *et al.* 2014; Cheng *et al.* 2016; Deepa and Dhepe 2014); ethanol (Cheng *et al.* 2012; Lee *et al.* 2016; Ye *et al.* 2012a, 2012b); isopropanol (Guo *et al.* 2021) and glycerol (Umar *et al.* 2022), in which no separate organic liquid product is explicitly mentioned without extraction of the product. It was assumed that a separate organic liquid could possibly be achieved, bearing in mind that using phenol as a capping agent in previous work in a continuous reactor working at 350 °C on the same softwood LignoBoost kraft lignin as in the present work yielded not only an aqueous and solid phase, but also a highly viscous organic phase (Belkheiri et al. 2018a, 2018b, 2016; Nguyen et al. 2014b). However, when lignin was depolymerised at the same reaction conditions without phenol, no liquid bio-oil phase was observed (Belkheiri *et al.* 2014) and it therefore seems that the formation of the highly viscous bio-oil phase found in the work of Belkheiri *et al.* and Nguyen *et al.* (Belkheiri *et al.* 2018a, 2018b, 2016; Nguyen *et al.* 2014b)

is dependent on the addition of phenol. Guaiacol, which was used in the current work, is structurally similar to phenol and yet no separate liquid organic bio-crude was produced when guaiacol was added: not even at the highest weight fraction added (2.2 wt%). However, there are some differences: the temperature in the works of Belkheiri *et al.* and Nguyen *et al.* was set at 350 °C; a continuous reactor was employed; salts based on potassium, rather than sodium, were used; and cooling on the flow line in the reactor was used instead of diluting the product in a cold trap after reaction (Belkheiri *et al.* 2018a, 2018b, 2016; Nguyen *et al.* 2014b). These differences in reaction conditions, particularly the dilution, could contribute to the explanation as to why phenol gave a separate oil phase and guaiacol did not.

The pH of the reaction mixture could not be measured precisely because final mixing of the pre-charge and the injection charge, which form the reaction charge, occurred inside the reactor. However, measurements made on mixtures with compositions equal to the reaction mixtures showed the pH to range between 10.7 and 12.7 for samples with NaOH added, and between 10.0 and 10.3 without NaOH added. The pH of the product mixture after dilution in the cold trap ranged between 9.9 and 10.9 with NaOH and 8.7-9.2 with no NaOH added. Although it is clear that a reaction mixture with a higher pH gave a product with a higher pH, the pH decreased during processing, which is in agreement with similar work (Belkheiri *et al.* 2016). Such decreases in pH may be caused by the formation of phenolic products during the depolymerisation, formation and dissolution of CO_2 and the formation of acids from the lignin during depolymerisation (Miller *et al.* 2002; Rößiger *et al.* 2018).

The reactor product (A), and the results of its fractionation, are shown in Figure 7. The aqueous suspension product (A) was filtered and the filter cake thus formed was dried to produce char (D). Acidification of the filtrate caused precipitation (B); after filtration, a clear liquid remained (C). The filter cake was dried and named precipitated solids (E). Drying the filtrate (C) produced ASO (F), a fraction in which the residual salts were found.

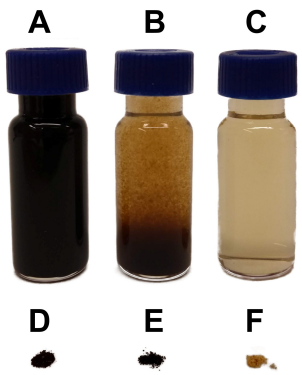

Figure 7: Fractions of the reaction product. Reactor product (A), acidified reactor product (B), filtrated acidified reactor product (C), char (D), precipitated solids, PS (E) and acid soluble organics, ASO (F).

Solid material was not formed in the control experiments without any lignin but with isopropanol and guaiacol present. Moreover, no material was precipitated from the product of the control experiments without lignin when the pH was lowered to 1.5. Thus, the char and PS fractions indeed originate from the lignin and not the capping agents reacting with themselves forming a solid phase or molecules precipitating after lowering the pH. This concurs with similar experiments in which phenol was used as the capping agent (Belkheiri *et al.*

2018a). However, guaiacol was seen to polymerise into a soluble component and ending up in the ASO fraction, see Paper IV: this fraction had a high molecular weight but remained soluble. Polymerisation of guaiacol to char has been reported in supercritical water as well as under pyrolysis conditions (Lawson and Klein 1985; Wahyudiono *et al.* 2011, 2007), yet, no char was formed from guaiacol under subcritical conditions at 250 °C (Wahyudiono *et al.* 2011). This is similar to the present work: while guaiacol polymerises when employing subcritical water, the polymerised material does not form a char fraction like it does in supercritical water.

4.1.1 Changes in molecular structure and weight

Investigation of the lignin with a light microscope, equipped with a heating plate, showed that it melted at around 190 °C. The solid products, char and PS did not, however, display any similar melting tendencies when heated up to 375 °C. The different melting properties strongly indicated that the molecular structure of the products differs from that of the lignin. Also, elemental analyses showed that the PS and char fractions had a higher carbon content than the original lignin, see Paper I, which, along with the general scope of this thesis, called for further characterisations of the material: NMR analyses, as well as determination of molecular weight of the products, were therefore undertaken.

At the outset of the work on NMR, the paper by Mattsson *et al.* (2016) was used as a starting point, since they have annotated the inter-unit ether linkages in the HSQC spectra of LignoBoost softwood kraft lignin. The inter-unit aliphatic region of the HSQC spectra of the LignoBoost lignin used in the present study is shown in Figure 8. Inter-unit ether linkages in the lignin are found, although many of them should have already been cleaved in the kraft pulping process (Lancefield *et al.* 2018). Mattsson *et al.* (2016) showed that these remaining inter-unit ether linkages were cleaved during depolymerisation under hydrothermal conditions at 350 °C, with phenol added as a capping agent and a residence time of 11 min: the signals for inter-unit ether linkages in lignin were lost in the products of Mattsson *et al.* (2016).

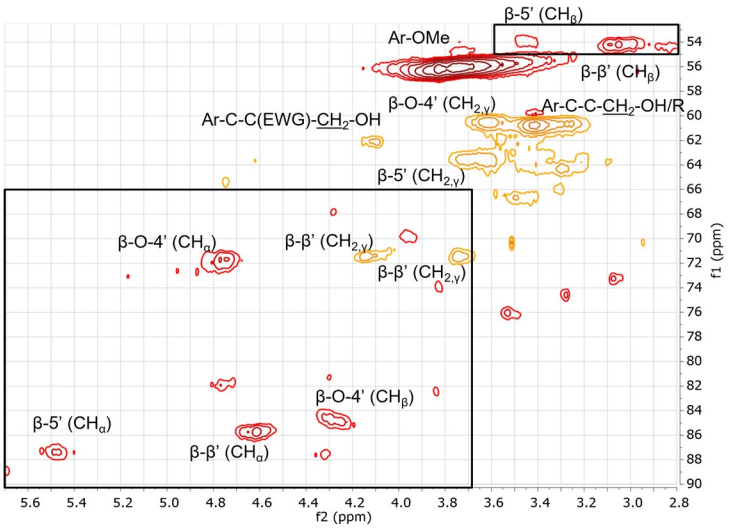

Figure 8: Inter-unit aliphatic region of the HSQC spectrum of the LignoBoost kraft lignin used in this study. Annotations of peaks are according to Giummarella et al. (2020) *and Mattsson et al.* (2016). *EWG: electron withdrawing group. The spectrum was run in an edited fashion: red peaks are CH and CH_3 groups and yellow peaks are CH_2 groups. Peaks from inter-unit ether linkages are enclosed in black rectangles.*

Analyses of the char and PS using HSQC showed that residual inter-unit ether linkages in the lignin structure disappeared completely during hydrothermal processing, see Papers I-IV. At first, this was found for samples run in the reactor with a residence time of 12 min and an average reaction temperature of 321 °C, see Paper I, very similar to the work of Mattsson *et al.* at 350 °C (Mattsson *et al.* 2016). However, studies using model compounds suggest that the cleavage of the important β-O-4' bond in lignin could be a rapid procedure, occurring within minutes in supercritical methanol (Tsujino *et al.* 2003). Abdelaziz *et al.* showed that an ethyl acetate extract of kraft lignin that was depolymerised for mere minutes was devoid of β-O-4' (Abdelaziz *et al.* 2018). They did not, however, report data on solid fractions after depolymerisation: such data was reported by Adamovic *et al.* (2022), who depolymerised kraft lignin in super-critical water (385 ± 1 °C, 254 ± 2 bar) for ultra-short residence times of 370 ± 30 ms. In their work, the inter-unit linkages remained in the solid residue after reaction (Adamovic *et al.* 2022).

The flexibility of the reactor used in the present work, coupled with its swift heating, allowed relatively short residence times, as low as 1 min, to be investigated. Capturing the effects that occur in the early phases of the residence in the reactor was optimised by using a lower reaction temperature of 290 °C, based on the hypothesis that reactions would be slower at a lower temperature. As was commented upon in chapter *3 Methods and Materials*, the injection of material and ensuing temperature drop made it difficult for a precise temperature to be reached or held, and the average temperatures therefore ranged between 270 and 301 °C. A range of residence times was investigated, with the shortest time being 1 min after completion of the injection, see Papers II-IV. Examples of the inter-unit aliphatic region of the HSQC spectra of the char and PS fraction for the T_{avg} of 291 °C and 1 min of residence time with 2.1 wt% guaiacol in the feed are presented in Figure 9. It is notable that the black rectangles, in which inter-unit ether linkages show up if they are present, see Figure 8, are empty for the char fraction (Figure 9A) and only show the faintest of peaks for the PS fraction (Figure 9B), suggesting these linkages have been cleaved already at this short residence time. The weak peaks within the black rectangle in Figure 9B disappear at longer residence times. A loss in inter-unit ether linkages was not only seen when guaiacol was used as a capping agent, but also for isopropanol and glycerol, see Papers II and III. This shows that rapid depolymerisation of the lignin is occurring under these reaction conditions. In the absence of a capping agent, no char was formed after 1 min residence time, but the PS fraction formed in that case had no inter-unit linkages present, see Paper IV, suggesting that lignin depolymerisation is also rapid when no capping agent is used.

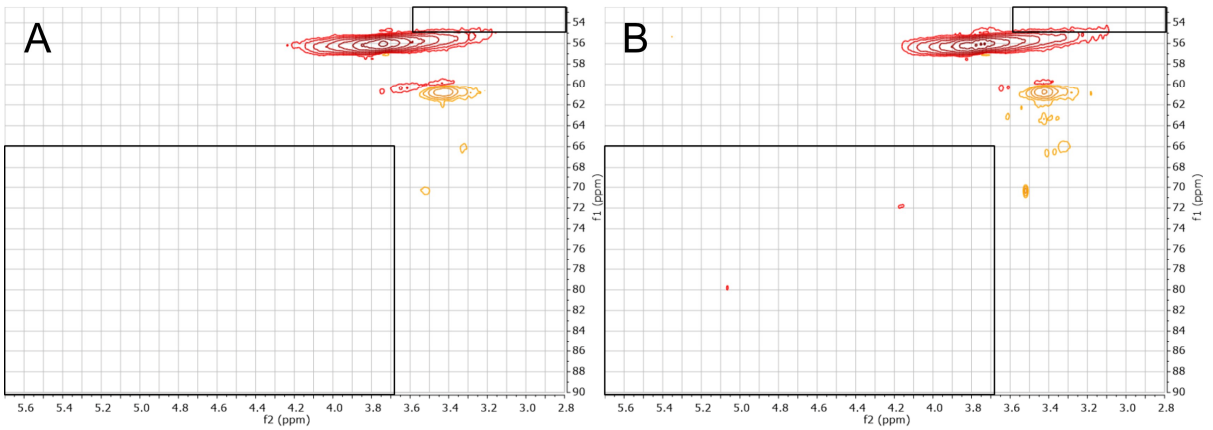

Figure 9: Inter-unit aliphatic regions of the HSQC spectra of char (A) and PS (B) at 1 min of residence time with 2.1 wt% guaiacol in the reactor feed and T_{avg} = 291 °C. N.B. The black rectangles, in which inter-unit ether linkage signals appear, are empty.

The molecular weights of the char and PS fractions were investigated using gel permeation chromatography (GPC). Figure 10 presents the molecular weight distributions for char, PS and ASO after 1 min of residence in the reactor and at an average reaction temperature of 276 °C. The capping agent used in this case was isopropanol and the weight fraction in the feed was 14 wt%, see Paper II.

The molecular weight distribution in particular changes rapidly, as large molecular weight fractions (>50 kDa) are lost already within the first minute of residence time, which is discussed in the section *4.2 Impact of residence time*. Similar results were seen for additions of glycerol, see Paper III, and guaiacol, see Paper IV, as well as with no capping agent, see Paper IV. The investigation of the molecular weights confirmed the results obtained from HSQC: the lignin depolymerises quickly and the fractions with the largest molecular weights disappear. Thus, it can be concluded that depolymerisation of the lignin occurs within 1 min of residence time, once injection is complete at the conditions investigated in this work, see Table 3. Furthermore, while the char and PS have similar molecular weight distributions, the ASO is quite different: this is in line with expectations that the ASO phase is comprised of smaller, soluble molecules.

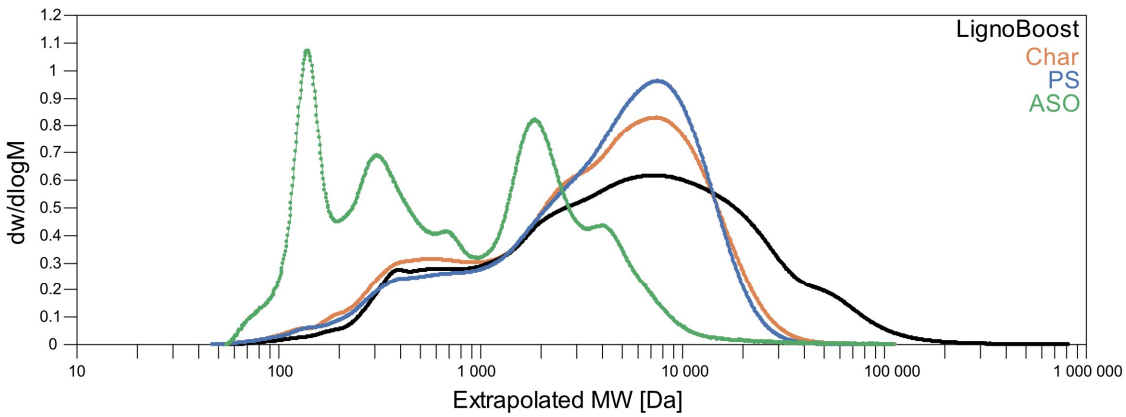

Figure 10: Molecular weight distributions of char, PS and ASO at 1 min of residence time after injection, at an average reaction temperature of 276 °C and with 14 wt% isopropanol in the feed.

4.1.2 Repolymerisation of reactive components

It is known that depolymerisation of lignin is often followed by repolymerisation, forming soluble higher M_w components and/or increasing the char yield (Abdelaziz *et al.* 2018; Adamovic *et al.* 2022; Pérez *et al.* 2022). High molecular weight fractions persisting after reaction could thus be repolymerised material. Repolymerisation of the reaction products was investigated primarily by examining their molecular weights; this will be discussed further later on in this chapter.

Among the reactions that can cause repolymerisation is the formation of diphenylmethanes, with formaldehyde being released from the lignin (Adamovic *et al.* 2022). In the present work, HSQC showed no evidence of diphenylmethanes being present in the LignoBoost kraft lignin, similar to other kraft lignins (Gellerstedt *et al.* 2004). However, following treatment in the reactor, some peaks for diphenylmethanes were observed, especially when guaiacol was used as the capping agent, but also without such an addition. All PS samples (with the exception of those from the run at 12 min with isopropanol) and some of the char fractions had these peaks, as shown in *Appendix II – Diphenylmethanes*, see Figure A6. Mattsson *et al.* found similar peaks in their lignin depolymerisation at 350 °C with phenol added as a capping agent (Mattsson *et al.* 2016) but only in the light oil phase, i.e. the DEE-solubles, and not in the solid product fraction. They suggest that formaldehyde released from the lignin side chain, by C_γ-C_β scission, could link the phenol added to their reaction mixture. A similar mechanism could potentially be in operation on the added guaiacol in the present work, along with aromatic rings in the liberated monomers, and also in the depolymerised lignin structure.

4.1.3 Precipitation of char and PS from the product mixture

The char fraction is defined in this work as the solids in the products mixture that has precipitated either during hydrothermal treatment or in the subsequent quenching of the reaction; the PS fraction, however, precipitates upon acidification to pH 1.5. An investigation, combining ATR-FTIR and NMR measurements, was undertaken to shed some light over these different precipitation behaviours since they affect the subsequent yields of the products.

Figure 11 shows the ATR-FTIR measurements obtained for the products formed with the addition of isopropanol. The PS fraction contains hydroxyl groups, resonating at 3042-3695 cm^{-1} (Faix 1992), and carbonyl units, resonating around 1700 cm^{-1}. The ASO fraction also display these carbonyl peaks. The char fraction, on the other hand, does not show any clear peak for carbonyl moieties, which might explain, in part, why it precipitates after reaction, see Figure 11. The ATR-FTIR analysis was only carried out on the products obtained from the reactions with isopropanol in the reaction feed, see Papers I and II. It is assumed, however, that the conclusions reached in this study also apply to the cases where glycerol and guaiacol replaced isopropanol as the capping agent, i.e. the char and PS have different functional groups.

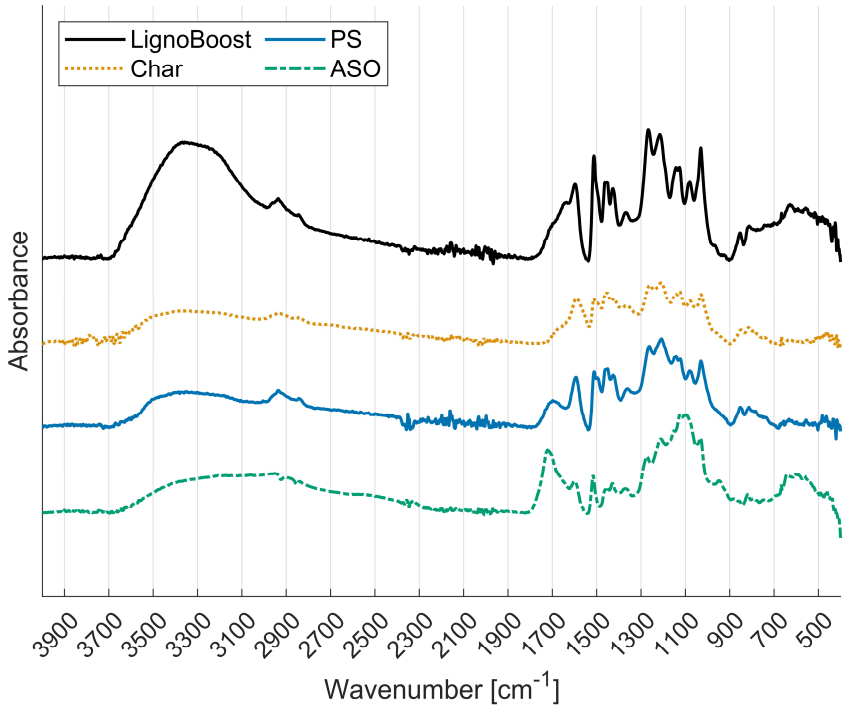

Figure 11: ATR-FTIR spectra of the product fractions after 1 min of residence time at $T_{avg} = 276$ °C with 14 wt% isopropanol in the reaction mixture feed.

Heteronuclear multiple bond correlation (HMBC) spectra were recorded to probe further into the nature of the carbonylic carbons found in the PS in Figure 11. The HMBC spectra for LignoBoost lignin and PS are presented in Figure 12.[2] Signals for carbonylic carbon showed in the HMBC spectra; indeed, signals corresponding to carboxylic acids and esters were found and are marked with black rectangles according to the annotations of McClelland *et al.* (2017).

[2] The HMBC spectra obtained for the char fraction were not clear and are thus not shown. This was probably due to the char agglomerating, which quenched the signal.

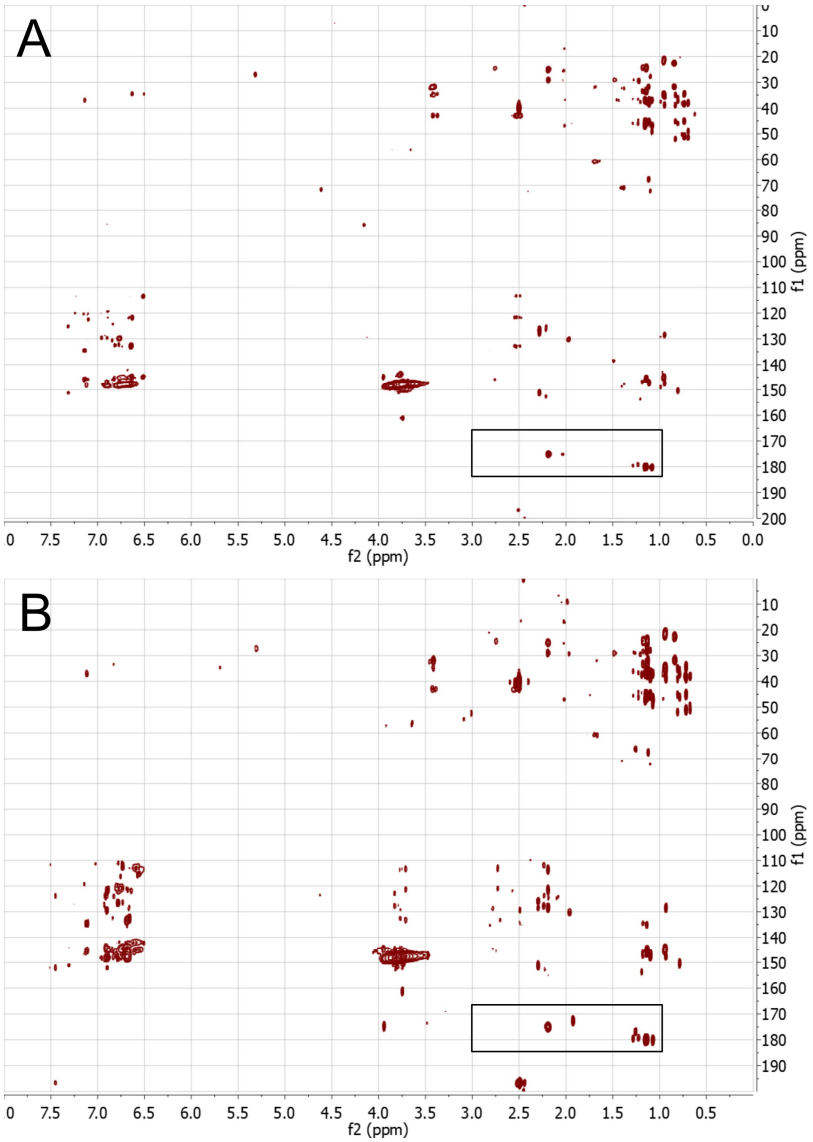

Figure 12: HMBC spectra of LignoBoost lignin (A) and PS after 4 min of reaction, with 13 wt% isopropanol in the feed and an average reaction temperature of 289 °C (B). The peaks within the black rectangles correspond to carboxylic acids and esters (McClelland *et al.* 2017).

Furthermore, the ^{1}H NMR spectra of the PS showed a broad peak between 12 and 13 ppm, which is typical of carboxylic acids, see Figure 13. Although the spectra in Figure 13 were recorded for a PS run with a residence time of 12 min, see Paper I, the same peaks were seen in the PS samples run at 4 min, i.e. the samples investigated by HMBC. No such peaks for carboxylic acids were seen in the char fractions.

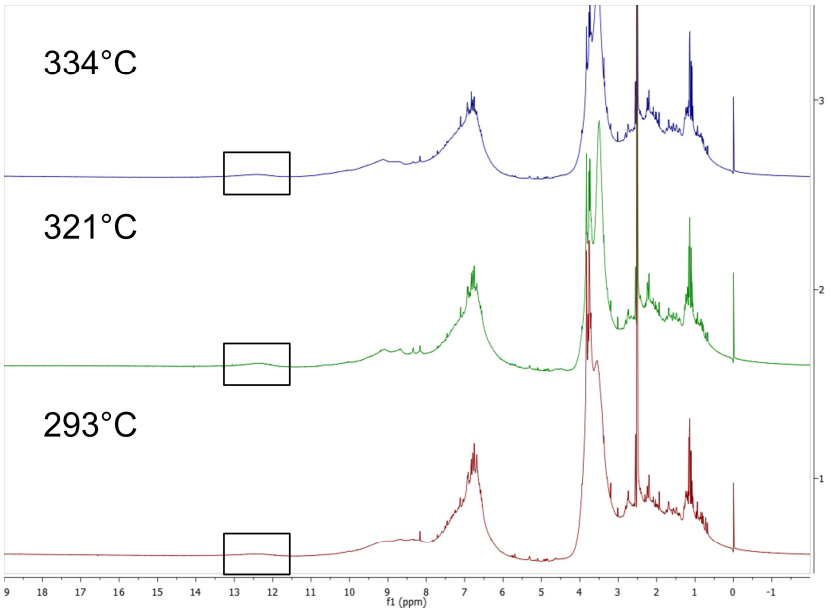

Figure 13: ^{1}H-NMR spectra of the PS run for 12 min at various average reaction temperatures, with 13-15 wt% isopropanol added to the feed.

The results of the ATR-FTIR, HMBC and ^{1}H NMR analyses show that functional groups differ in the products, and this can at least partly explain the different precipitation behaviours. The PS and ASO appear to have polar functional groups that keep them dissolved in the aqueous product phase, whilst the char, having less or none of these groups, precipitates.

4.1.4 Monomers formed

In the GC-MS analysis it was found that water-soluble monomers were present in the diethyl ether extract of the ASO phase. Control experiments on dissolved and extracted lignin showed no monomers, proving that the monomers identified were indeed the result of the hydrothermal treatment, see Paper IV. A typical result of the GC-MS analysis is presented in Figure 14 for a sample run at 12 min of residence time, see Paper I. The products identified are clearly aromatic; many are also phenolic. It is notable that the major monomeric product identified in the figure was guaiacol **(2)**. This is in agreement with the softwood lignin used, which is rich in guaiacyl units (Abdelaziz *et al.* 2018; Gellerstedt 2015). 4-methyl guaiacol and catechol were not separated adequately, so the detected catechol therefore contains an unquantified amount of 4-methyl guaiacol **(4a)**. Moreover, it was noted that catechol was not formed at shorter residence times, see Papers II-IV. Instead, it required longer residence times in order to form, see Paper IV, which concurs with the findings of Pérez *et al.* (Pérez *et al.* 2022).

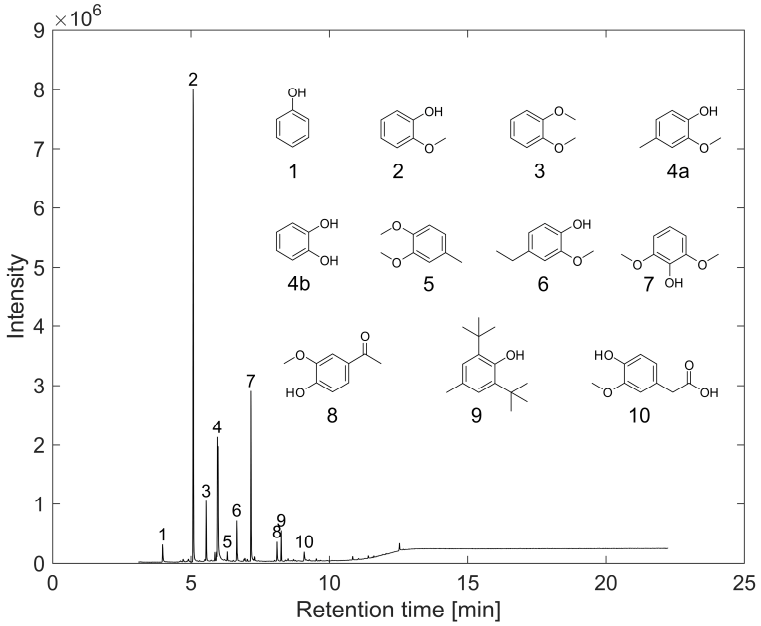

Figure 14: Typical GC-MS spectra for samples run at 12 min, at T_{avg} = 321 °C with 13 wt% isopropanol in the feed. 1) phenol, 2) guaiacol, 3) 1,2-dimethoxybenzene (veratrole), 4a) 4-methyl guaiacol, 4b) catechol, 5) 3,4-dimethoxy toluene (homoveratrole), 6) 4-ethyl guaiacol, 7) syringol, 8) apocynin, 9) BHT and 10) homovanillic acid. Syringol (7) is the internal standard and BHT (9) is a preservative in the solvent. The peak (4) is a mixture of 4-methyl guaiacol (4a) and catechol (4b).

4.2 Impact of residence time

The effect of changing residence time in the reactor was investigated with additions of isopropanol, glycerol, guaiacol and with no capping agent added. Residence times of 1, 2, 4 and 12 min were investigated for isopropanol and glycerol; the residence time of 2 min was omitted for guaiacol. Only 1 and 4 min of residence times were investigated in the case without a capping agent, where it was found that no char was formed at 1 min.

4.2.1 Effect on molecular weight

The M_w of the product fractions obtained at various residence times and additions of capping agent are reported in Table 5. The values of the M_w measured for the LignoBoost lignin differ slightly between the different studies, likely due to the instrument being recalibrated in between studies. It is well-known that it is difficult to perform precise molecular weight measurements on lignin (Zinovyev *et al.* 2018). Comparisons of the effect of increasing residence time within the respective series can nevertheless be made.

Inter-unit ether linkages were cleaved already within the first minute of residence time, as shown in the section *4.1.1 Changes in molecular structure and weight*, and the molecular weight distribution changed significantly from the original lignin. As such, the product fractions all have a lower M_w than the original lignin and an altered molecular structure.

Table 5: Weight average molecular weight (M_w) of the product fractions at different additions of capping agent and residence times. Isopropanol: T_{avg} = 276-292 °C, with 12-14 wt% isopropanol in the feed and no added NaOH. Glycerol: T_{avg} = 270-291 °C, with 15-17 wt% glycerol and 1 wt% NaOH in the reaction feed. Guaiacol: T_{avg} = 291-301 °C, with 2.1-2.2 wt% guaiacol and 1 wt% NaOH in the reaction feed. No capping agent: T_{avg} = 288-294 °C, with 1 wt% NaOH in the feed. Standard deviations are given where multiple runs were made in the reactor.

	LignoBoost [kDa]	Product fraction	1 min	2 min	4 min	12 min
Isopropanol	12.2 ± 0.4	Char [kDa]	5.9	5.4	4.7	6.1
		PS [kDa]	5.9	4.6	4.5	4.7
		ASO [kDa]	1.7	1.3	1.2	1.3
Glycerol	13.2 ± 0.3	Char [kDa]	11.5 ± 0.6	11.6	8.8 ± 0.1	6.8
		PS [kDa]	8.5 ± 0.7	7.6	7.5 ± 0.3	5.9
		ASO [kDa]	0.9 ± 0.0	0.9	0.8 ± 0.0	0.9
Guaiacol	11.8 ± 0.1	Char [kDa]	3.6	--	3.7 ± 0.4	4.7
		PS [kDa]	5.5	--	6.3 ± 0.2	6.6
		ASO [kDa]	1.5	--	2.1 ± 0.1	2.0
No capping agent	11.8 ± 0.1	Char [kDa]	--	--	7.0 ± 0.4	--
		PS [kDa]	7.9	--	7.8 ± 0.2	--
		ASO [kDa]	1.3	--	1.5 ± 0.1	--

The effect that increasing residence time has on the M_w of the reaction product fractions depends on the capping agent used. In the case of isopropanol, an increase in residence time initially causes depolymerisation to progress, which reduces the M_w of all products fractions, see Table 5. Between 4 and 12 min of residence time, however, a net repolymerisation occurs as the M_w increases again. Competing reactions that depolymerise and repolymerise the reactor content between 4 and 12 min of residence time thus favour a net repolymerisation after 4 min. Similar repolymerisation can be seen when guaiacol is used as the capping agent, see Table 5, although somewhat less clearly. Repolymerisation reactions overtake the depolymerisation reactions between 4 and 12 min of residence time for the char fraction, whereas they start earlier for the PS fraction. Such a consecutive model of reaction, with initial rapid depolymerisation followed by slower repolymerisation, has been noted previously (Bobleter and Concin 1979; Roberts *et al.* 2011; Zhang *et al.* 2008).

When glycerol is the capping agent, on the other hand, the M_w decreases monotonously. This is shown in Figure 15, where the molecular weight distributions from which the M_w of the glycerol series in Table 5 are calculated, are presented. The reason why the addition of glycerol caused a different behaviour with increasing residence time compared to the other capping agents was not investigated further.

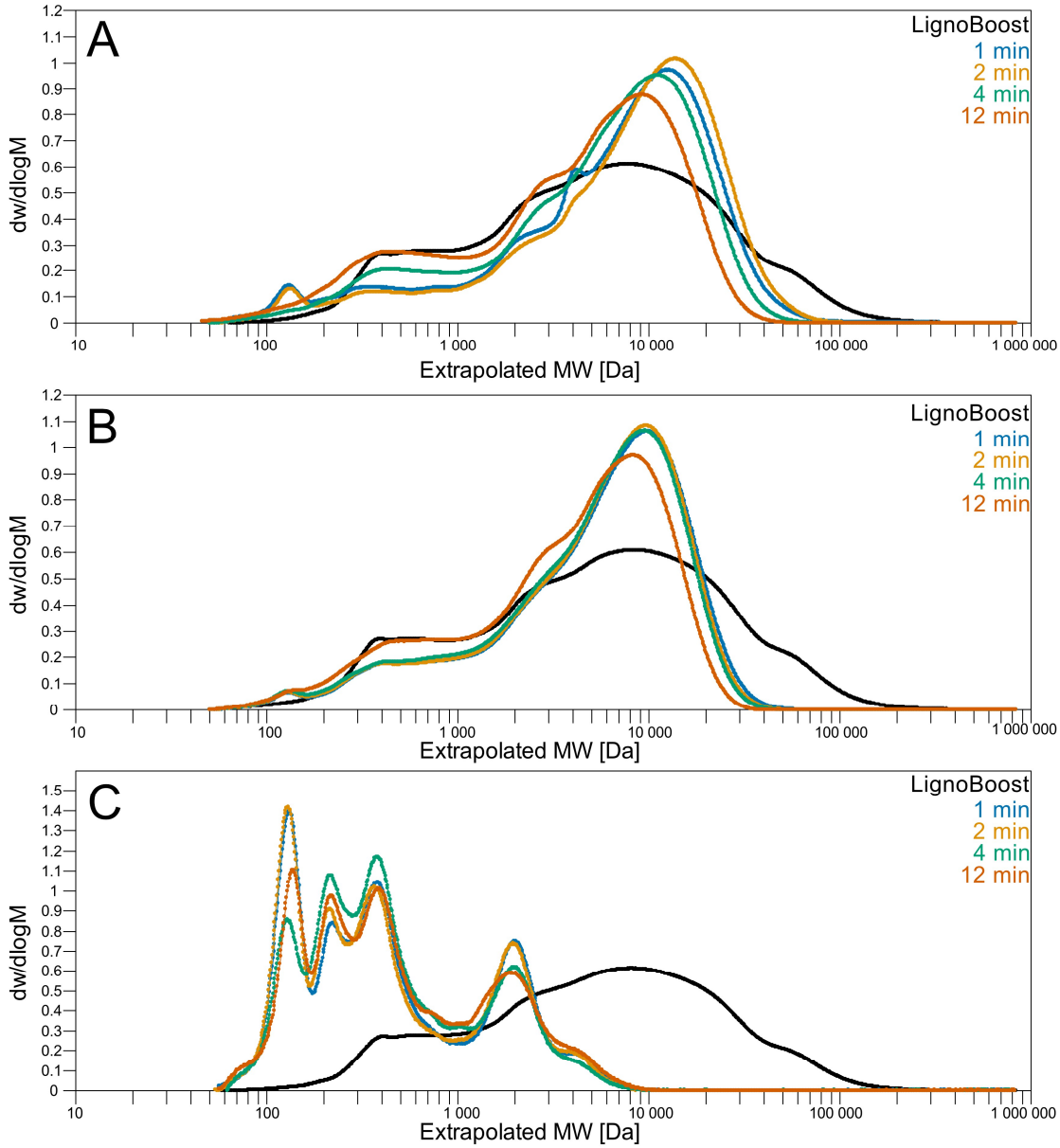

Figure 15: Molecular weight distributions of char (A), PS (B) and ASO (C) at different residence times with the addition of 15-17 wt% glycerol and T_{avg} = 270 to 291 °C.

4.2.2 Effect on yields of products

The yields of the product fractions char, PS and ASO vs. residence time when different capping agents were used are presented in Figure 16. The major product formed in all cases is the precipitated solids, PS. The yield of this fraction decreases a little with increasing residence time but, in all cases, remains the major product even after 12 minutes of residence time. The yield of the ASO fraction can be seen to increase somewhat with residence time in all cases when a capping agent is used, but decrease when no capping agent is present, Figure 16D.

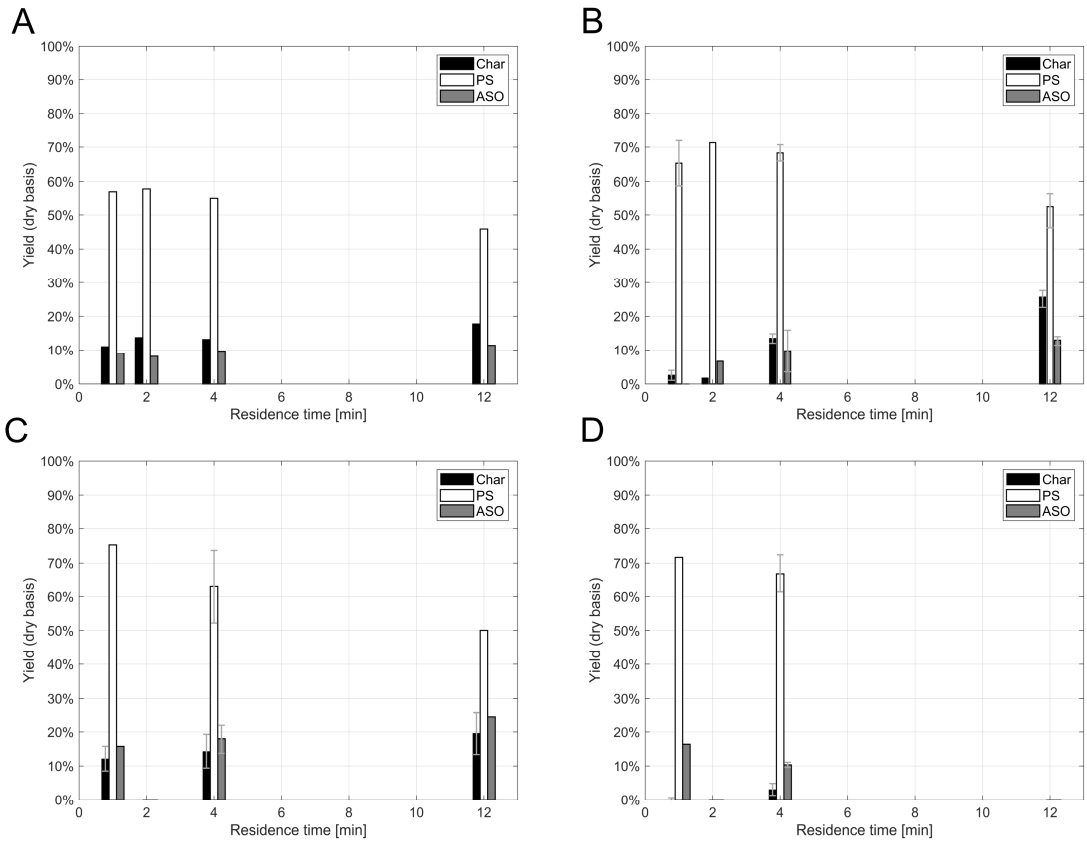

Figure 16: Yields of product fractions vs. residence time at different additions of capping agent. (A): 12-14 wt% isopropanol, T_{avg} = 276-292 °C and no added NaOH. (B): 15-17 wt% glycerol, T_{avg} = 270-291 °C and 1 wt% NaOH. (C): 2.1-2.2 wt% guaiacol, T_{avg} = 291-301 °C and 1 wt% NaOH. (D): no capping agent, T_{avg} = 288-294 °C and 1 wt% NaOH. Standard deviations are marked with error bars for cases with multiple reactions run at the same conditions. The amount of lignin injected was uncertain at the 12 min reactor run in (B) and the error bars cover this uncertainty, see Paper III. The char yield in (C) and (D) was determined after dividing the product charge in two; the error bars show the standard deviation of the average of these two reactor runs, see Paper IV.

Upon increasing the residence time, the trend is that the yield of char increased but to different degrees, depending on the conditions and capping agents: it is possible that this increase is due to repolymerisation or condensation of the material in the reactor, which causes more char to form (Gosselink *et al.* 2012; Zhang *et al.* 2008). However, in many instances, this increase in yield is accompanied by a decrease in $M_{w,}$ as shown in Table 5. The solubility of the char in the product phase, which ultimately determines its yield, thus appears to be dependent on more factors than just the molecular weight, e.g. the content of functional groups such as carboxylic acids, which was discussed in the section *4.1.3 Precipitation of char and PS from the product mixture*. Furthermore, the molecular weight is about the same for both the PS and char fractions, as reported in Table 5. This implies that the difference in solubility between these two phases depends, to a large degree, on the type of functional groups in the molecular structure and not only the molecular weights. As mentioned above, the yield of the PS fraction decreases, and the yield of the char fraction increases, with increasing residence time. A hypothesis can thus be put forward that, at longer residence time, the fragments from the lignin that was depolymerised initially and would form a PS fraction, lose functional groups at longer residence times: they transform from PS, which remain dissolved after reaction, into

char, which precipitates. It is also possible that some of the increase in char yield comes from fragments of low molecular weight compounds in the PS or ASO fraction that react and become hydrophobic so that they precipitate. The net effect of this would be a decrease in the average M_w of the char while its yield increases simultaneously.

4.2.3 Formation of monomers

The yield of monomers vs. dry lignin added to the reactor, as identified and semi-quantified by GC-MS, increased with residence time with the exception of vanillin and apocynin, both of which decreased, see Figure 17. The main product is guaiacol, as can be seen in Figure 14. Typically, in hydrothermal studies, the yield of guaiacol reaches a maximum after which it decreases with increasing residence time, e.g. the work of Roberts *et al.* at 300 °C, who used organosolv lignin with 2 wt% NaOH, where a maximum of guaiacol was detected at 5 min residence time (Roberts *et al.* 2011). After 5 min, they found that the guaiacol reacted further and the yield decreased with increasing residence time. This is not the case in the present work, however, because the guaiacol yield increased with residence time: whether this is an effect of using a different type of lignin, base concentration or reactor set-up is unknown. Longer residence times could potentially have caused a decrease in guaiacol in this work: Dunn and Hobson noted that the portion of guaiacol formed is highest at short residence times (Dunn and Hobson 2016). Alkyl guaiacols are formed to a larger extent at longer residence times, see Figure 17.

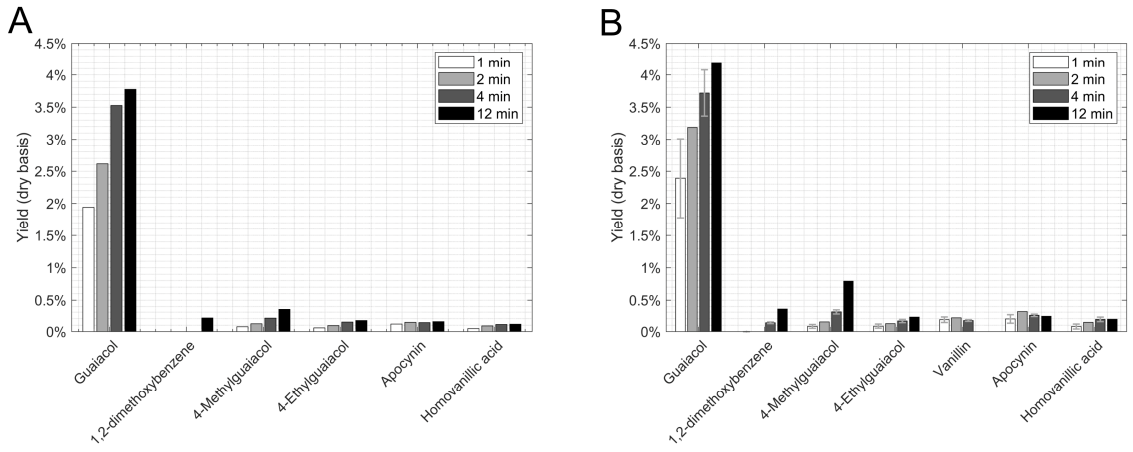

Figure 17: Semi-quantified yields of the monomers identified with GC-MS vs. dry lignin added to the reactor. (A): 12-14 wt% isopropanol, T_{avg} = 276-292 °C and no NaOH added, see Paper II. (B): 15-17 wt% glycerol, T_{avg} = 270-291 °C and 1 wt% NaOH, see Paper III.

The investigations reported in Paper IV relate the effects that increasing residence times have on monomer yields without a capping agent and with 2.2 wt% guaiacol added, respectively. They show that without an addition of guaiacol, the trends are the same as those seen in Figure 17, i.e. at longer residence times, the yields of all components increase except for apocynin and vanillin. However, with guaiacol added to the reaction mixture, the yield of monomers is much higher than in the case without a capping agent: some of these monomers could be derived from this added guaiacol. With guaiacol added the trend of the guaiacol yield is reversed: an increased residence time causes a decrease in the amount of guaiacol identified.

The net effect of the treatment is a consumption of guaiacol that increases with increasing residence time.

4.3 Impact of temperature

Some comments on the effect of reaction temperature are presented here. Increasing the reaction temperature from 290 to 335 °C, corresponding to average temperatures of 293-334 °C had a similar effect on the yields as increasing the residence time: it shifted the yield from PS to char, see Paper I. With increasing temperature, the M_w of the char is also reduced while that of the PS fraction is increased, see Table 6.

Table 6: Weight average molecular weight (M_w) of the product fractions at 12 min of residence time, with 13-15 wt% isopropanol and no NaOH in the reaction feed.

T_{avg} [°C]	Char [kDa]	PS [kDa]	ASO [kDa]
LignoBoost	11.4 ± 0.1		
293 °C	4.9	6.0	1.4
321 °C	4.0	6.4	1.7
334 °C	3.9	6.8	1.9

Furthermore, the elemental composition of the char fraction changed with increasing temperature. While the carbon content of the original lignin was 68.0 wt% ± 0.0 wt%, the char fraction obtained at an average temperature of 293 °C displayed an increased carbon content: 70.1 wt% ± 0.0 wt%. At an even higher average temperature, 334 °C, the carbon content in the char increased to 76.1 wt% ± 0.1 wt%. While the hydrogen content of the char fraction remained stable, and the amount of sulphur was too low to quantify accurately, it is suggested that this increase in the carbon content of the char was accompanied by a reduction in the oxygen content: from 24.9 wt% ± 0.7 wt% to 18.7 wt% ± 0.0 wt%. Similar trends, with increasing carbon contents and reduced sulphur contents with increasing temperature, were reported for the oil phase when LignoBoost lignin was depolymerised using phenol as a capping agent (Nguyen *et al.* 2014a).

4.4 Impact of capping agents

Two of the studies in this thesis report the findings of varying the concentrations of capping agent in the feed, namely those on isopropanol and guaiacol in Papers I and IV, respectively. Furthermore, a control test in the glycerol study also provides information on the effect of using glycerol as a capping agent. It is not appropriate to directly compare the results of the different types of capping agent here: the reactions were run at different residence times and concentrations of capping agents, as well as with and without additions of NaOH. Trends within the studies are, however, investigated.

4.4.1 Effect on molecular weight

The M_w of the product fractions at increasing mass fractions of the capping agent are shown in Table 7. The residence times differ between the studies, yet the general trends shown for the additions of capping agents are similar: a decrease in the M_w of the char and the PS fractions is found with increasing amounts of isopropanol, glycerol and guaiacol in the reactor feed. It thus appears that the addition of either guaiacol, glycerol or isopropanol is able to

impede repolymerising reactions and is instrumental in the depolymerisation process. However, the effect of capping agents on the M_w of ASO components shows no evident trend: neither a monotonous increase nor a decrease.

Table 7: Weight average molecular weight (M_w) of the product fractions obtained using three different capping agents. Reactions where duplicate reactions were run are presented as averages with standard deviations. No char was formed at 0 wt% guaiacol in the feed at 1 min of residence time. Isopropanol: T_{avg} = 313-321 °C, with no added NaOH. Glycerol: T_{avg} = 281-290 °C, with 1 wt% NaOH in the reaction feed. Guaiacol at 1 min: T_{avg} = 291 °C, with 1 wt% NaOH in the reaction feed. Guaiacol at 4 min: T_{avg} = 288-301 °C, with 1 wt% NaOH in the reaction feed. Standard deviations are given where multiple runs were made in the reactor.

	Residence time [min]	LignoBoost [kDa]	Mass fraction of capping agent in the feed [wt%]	Char [kDa]	PS [kDa]	ASO [kDa]
Isopropanol	12	11.4 ± 0.1	0	8.2	8.3	1.7
			4	5.8	6.4	1.6
			13	4.0	6.4	1.7
			24	4.1	5.7	1.6
Glycerol	4	13.2 ± 0.3	0	10.1	8.7	1.2
			15	8.8 ± 0.1	7.5 ± 0.3	0.8 ± 0.0
Guaiacol	1	11.8 ± 0.1	0	--	7.9	1.3
			2	3.6	5.5	1.5
Guaiacol	4	11.8 ± 0.1	0	7.0 ± 0.4	7.8 ± 0.2	1.5 ± 0.1
			0.2	6.5	6.3	1.4
			1	4.2	6.1	1.5
			2	3.7 ± 0.4	6.3 ± 0.2	2.1 ± 0.1

4.4.2 Effect on the product yields

The yields of the product fractions obtained when varying amounts of isopropanol and guaiacol were added to the feed are presented in Figure 18. Different reaction temperatures, residence times and additions of NaOH were employed in these series, see Table 3; these reaction parameters influence the char yields, as shown in the sections above. Comparing the absolute levels of char is therefore not feasible, since factors other than the added capping agent affect the result. The trends with increasing levels of capping agent do, however, differ depending on the type of capping agent used. Increasing the amount of isopropanol, for example, caused a general decrease in the yield of char coupled with an increase in the yield of PS, see Figure 18A. The addition of guaiacol, on the other hand, showed an increase in the yield of char as the amounts added increased, see Figure 18B.

The addition of glycerol to the reaction mixture also caused an increase in the yield of char, as was the case with guaiacol, see Paper III. Some of this increase is due to residual glycerol being present in the char, since the filter cake was not washed. Even so, when this residual glycerol is discounted, the yield of char was higher when glycerol was added. Previous work on the addition of glycerol to the hydrothermal liquefaction of rice straw and aspen wood has shown that it could cause a decrease in the yield of char, but the reactions of such

carbohydrate-containing material are different to those of pure lignin (Kashimalla *et al.* 2021; Pedersen *et al.* 2015).

Finally, it was noted that adding NaOH to the reaction mixture indeed had an effect on the yield of char, see Paper III. The addition caused less char to form, though it is uncertain whether this is due to the increased solubility of products at higher pH in the product phase, or if the reactions were affected by the fact that a higher pH caused less char to be formed.

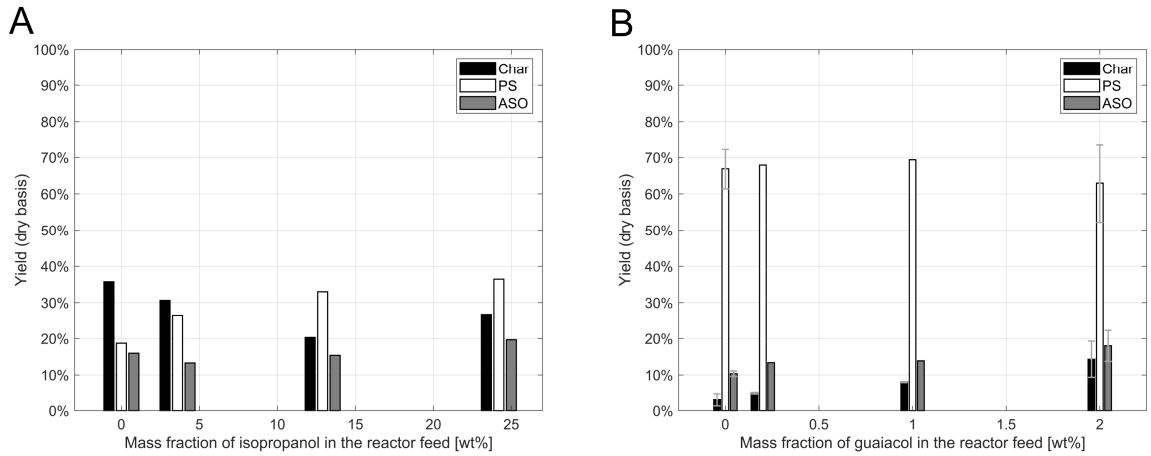

Figure 18: Yields of product fractions obtained with varying mass fractions of capping agent in the feed. (A): isopropanol at 12 min of residence and T_{avg} = 313-321 °C with no added NaOH. (B): guaiacol at 4 min of residence time at T_{avg} = 288-301 °C, with 1 wt% NaOH in the reaction feed

All the alcohols added, i.e. isopropanol, glycerol and guaiacol, thus affect the reactions and aid in reducing the M_w of the char and PS products and, as such, they work as capping agents. With respect to their ability in reducing the char yield, however, they differ. Isopropanol addition decrease the yield of char formed in this work, whereas guaiacol and glycerol increase the yield of char. It has been noted that isopropanol and glycerol can perform as hydrogen donors (Kim *et al.* 2014; Löfstedt *et al.* 2016; Pedersen *et al.* 2015; Yuan *et al.* 2007). In their review on co-solvents in the hydrothermal liquefaction of algae, Han *et al.* identify another effect of isopropanol, namely that it changes the physical properties of both the reaction mixture and the bio-oil (Han *et al.* 2020). They saw little improvement in yield and an almost constant H/C ratio, suggesting that little hydrogen transfer occurred. However, the physical properties (such as viscosity and aging) of the bio-oil they produced were improved when isopropanol was added (Han *et al.* 2020). The isopropanol added in the present work reduced not only the M_w of the char but also the amount that was formed and, as such, may be suitable for the process.

4.4.3 Formation of monomers

No major changes were found in the yields of monomers, semi-quantified by GC-MS, when the amount of isopropanol added was varied, see Paper I. While it was anticipated that monomers alkylated with isopropanol could form (Sato *et al.* 2002), no apparent propyl alkylated monomers from isopropanol alkylation were found in the present work, which concurs with the results of Schmiedl *et al.* (2012). Nevertheless, evidence of new structures was found as new peaks appeared in the HSQC spectra of char and PS when capping agents were added, which

suggests they form new bonds with the lignin products. However, the existence of such new bonds was not investigated further.

The effect of adding glycerol to the reaction mixture is a weak decrease in the monomer yield, see Paper III. The effect of adding guaiacol, however, is less clear. Evaluating the influence of guaiacol is very difficult, not only due to it being one of the major monomers produced during the operation, but also because it may also react and form other monomers. Consequently, it is impossible to fully estimate how much of the guaiacol originates from lignin and how much from the guaiacol added. However, adding guaiacol to the reaction mixture clearly affects the monomer yield, shown partly by the unreacted guaiacol that skews the result. When the guaiacol is deducted, the semi-quantified yield is still greater with guaiacol added to the feed, see Paper IV; at least some of this increase in monomer yield may be guaiacol in the feed that has formed other monomers during the experiment. Control experiments showed guaiacol to form 1,2-methoxybenzene when run in the reactor without lignin. It was also noted that adding NaOH to the reaction mixture increased the amount of monomers formed, see Paper III, possibly due to the higher pH of the reaction mixture.

5
Conclusions

This work has shown that the hydrothermal depolymerisation of softwood kraft lignin at 250 bar and temperatures ranging between 290 and 335 °C (corresponding to average temperatures 270-334 °C), with 1.6 wt% Na_2CO_3 and the addition of varying amounts of NaOH yields, at residence times of 1-12 min, an aqueous suspension without any liquid organic phase in it. The depolymerisation process is rapid, with inter-unit ether linkages, such as β-O-4', being cleaved within one minute of residence time in the reactor.

Additions of isopropanol, glycerol and guaiacol were made to investigate whether they could mitigate repolymerisation of the products obtained. Additions of all three compounds caused the molecular weights of the solid products of the depolymerisation, char and precipitated solids (PS) to decrease, and isopropanol caused the yield of char to decrease, too. Additions of glycerol or guaiacol, on the other hand, caused the yield of char to increase.

Increasing the residence time caused the char yield to increase, but also the apparent semi-quantified yield of monomers, the main one of which is guaiacol. The increase in residence time also caused more extensive depolymerisation, seen as a reduction in the weight average molecular weight (M_w). However, between 4 and 12 min of residence time, a net repolymerisation was discovered: an increase in the M_w was noted when isopropanol and guaiacol were added. With glycerol added, no net repolymerisation was observed for residence times up to 12 min. Although making comparisons between the different capping agents is difficult due to the varying reaction conditions, the rapid depolymerisation of lignin seen for all the capping agents added calls for careful adjustment of the residence time.

6
Future Work

The work presented in this thesis indicates that depolymerisation reactions are rapid. It also investigated the use of isopropanol, glycerol and guaiacol as capping agents. Some suggestions for further research are outlined below.

The focus in this work was short residence times and, consequently, no residence times exceeding 12 min were investigated. As the semi-quantified yield of monomers increased with residence time, investigating whether this trend remains at longer residence time could be of interest. It would also reveal if the char yield continues to increase at longer residence time or reaches a constant value instead. In addition, investigations tracking the carbon content of the elemental composition at increased residence time would provide information on the carbonisation of the products. In the glycerol series, the decrease in weight average molecular weight (M_w) of char and PS was monotonous over the entire range of residence times investigated, whereas a repolymerisation was observed for the other capping agents investigated. Whether repolymerisation of the products would begin at longer residence times remains an open question. Lastly, investigating even shorter residence times of under 1 min could show how quickly the inter-unit ether linkages are cleaved in the temperature range investigated in this work.

NaOH was not added to any of the cases in which isopropanol was used as a capping agent in this work, since the lignin dissolved satisfactorily with just Na_2CO_3 being added. It would, however, be of interest to investigate the effect an addition of NaOH has on the char yield, as this would allow the effect of isopropanol to be compared in more depth to that of guaiacol and glycerol.

Closer investigation of the molecules formed at the initial depolymerisation would provide greater clarification of their functional groups when bonds within the lignin break early in the reaction process. Knowledge pertaining to this could be used for designing more efficient capping agents. Also, the kinetics of the reactions could be investigated further, as in the work by Yong and Matsumura (2013).

Ether bonds in the lignin were shown to break in this work whilst C-C bonds mostly remained, keeping the M_w of the products fairly high: inexpensive catalysts that break these C-C bonds efficiently will therefore be required in order to increase the yield of monomers. Breaking C-C bonds would liberate larger amounts of low molecular weight material and indeed monomers, thus increasing the yield of products of higher value.

7
Acknowledgements

The financial support received from The Swedish Energy Agency for this work is gratefully acknowledged along with funding for conference participation from the Bo Rydin Foundation for Scientific Research and the Adlerbert Research Foundation.

Completing this journey would not have been possible without a number of people to whom I would like to extend my sincerest gratitude:

- First and foremost my main supervisor, Prof. Hans Theliander, for taking me on as a Ph.D. student and challenging me throughout these years. Thank you for the patience you showed as I constantly doubted the results.
- My co-supervisor, Assoc. Prof. Merima Hasani, who first invited me to SIKT and supported me continuously during this journey.
- Assoc. Profs. Marco Maschietti and Rudi Nielsen, for inviting me to Aalborg University in Esbjerg, Denmark, and providing me with both access to, and help with, the depolymerisation reactor, as well as your continuous support in co-authorship.
- Ms. Dorte Spangsmark and Dr. Nikolaos Montesantos for their assistance in the lab at Aalborg University in Esbjerg.
- Dr. Huyen Lyckeskog for help and introductions to the subject of kraft lignin depolymerisation.
- Dr. Cecilia Mattsson for initiating this project.
- Mr. Michael Andersson-Sarning for his excellent help with maintenance of the instruments. Ms. Ximena Rozo Sevilla for all help with lab technicalities.

- ❖ Former Ph.D. students at SIKT, now doctors: Maria Gunnarsson (also for NMR support), Beatrice Swensson, Joanna Wojtasz-Mucha, Anders Åkesjö, Erik Karlsson and Axel Martinsson, for leading the way.
- ❖ Dr. Tor Sewring for all his help when I began as a Ph.D. student, and to Mr. Kenneth Gacutno Arandia for being such excellent office friends.
- ❖ Ms. Malin Larsson for her excellent administrative support and continuous encouragement.
- ❖ Ms. Anna Hjorth and Mr. You Wayne Cheah for making the teaching of transport phenomena such delight, as well as outstanding encouragement during these years, and especially so during the dreadful pandemic years.
- ❖ Dr. Aleksandra Kozlowski, Ms. Shirin Naserifar, Ms. Carolina Marion de Godoy, Mr. Linus Kron, Ms. Emma Månsson, and Ms. Amanda Sörenssen Ristinmaa for such wonderful encouragement.
- ❖ Assoc. Prof. Diana Bernin for clarifying NMR discussions. Also, Dr. Ulrika Brath and Dr. Zoltan Takacs, and the staff at the Swedish NMR Centre, for their skilful help with the NMR measurements.
- ❖ Dr. Stellan Holgersson for sharing his skill in making ICP-OES measurements, and Dr. Stefan Gustafsson at CMAL for his help with the CHNS measurements.
- ❖ Assoc. Prof. Sven-Ingvar Andersson for teaching me the AAS and for his input in terms of discussions and help with mending the larger scale reactor together with Mr. Ulf Stenman.
- ❖ All colleagues, former and present, at SIKT and KART, including Dr. Nabin Karna & Dr. Probal Basu.
- ❖ The staff at the Chalmers Library for expedient service in finding old references.
- ❖ Ms. Maureen Sondell for her excellent linguistic review.
- ❖ Ms. Frida Björklund for the cover figure.
- ❖ All members of the local Ph.D. council at K and Bio for their continuous work aimed at improving the circumstances of Ph.D. students.

Last, but definitely not least: friends and family, for your truly remarkable support throughout this journey, not the least during the COVID-19 pandemic. This would not have been possible without you!

Thank you all!

8

References

Abad-Fernández, N., Pérez, E., Martín, Á. and Cocero, M.J. (2020). Kraft lignin depolymerisation in sub- and supercritical water using ultrafast continuous reactors. Optimization and Reaction Kinetics. J. Supercrit. Fluids 165: 104940. https://doi.org/10.1016/j.supflu.2020.104940

Abdelaziz, O.Y. and Hulteberg, C.P. (2020). Lignin Depolymerization under Continuous-Flow Conditions: Highlights of Recent Developments. ChemSusChem 13: 4382–4384. https://doi.org/10.1002/cssc.202001225

Abdelaziz, O.Y., Li, K., Tunå, P. and Hulteberg, C.P. (2018). Continuous catalytic depolymerisation and conversion of industrial kraft lignin into low-molecular-weight aromatics. Biomass Convers. Biorefinery 8: 455–470. https://doi.org/https://doi.org/10.1007/s13399-017-0294-2

Abdelaziz, O.Y., Meier, S., Prothmann, J., Turner, C., Riisager, A. and Hulteberg, C.P. (2019a). Oxidative Depolymerisation of Lignosulphonate Lignin into Low-Molecular-Weight Products with Cu–Mn/δ-Al2O3. Top. Catal. 62: 639–648. https://doi.org/10.1007/s11244-019-01146-5

Abdelaziz, O.Y., Ravi, K., Mittermeier, F., Meier, S., Riisager, A., Lidén, G. and Hulteberg, C.P. (2019b). Oxidative Depolymerization of Kraft Lignin for Microbial Conversion. ACS Sustain. Chem. Eng. 7: 11640–11652. https://doi.org/10.1021/acssuschemeng.9b01605

Adamovic, T., Zhu, X., Perez, E., Balakshin, M. and Cocero, M.J. (2022). Understanding sulfonated kraft lignin re-polymerization by ultrafast reactions in supercritical water. J. Supercrit. Fluids 191:. https://doi.org/10.1016/j.supflu.2022.105768

Adler, E. (1977). Lignin chemistry—past, present and future. Wood Sci. Technol. 11: 169–218. https://doi.org/10.1007/BF00365615

Arturi, K.R., Strandgaard, M., Nielsen, R.P., Søgaard, E.G. and Maschietti, M. (2017). Hydrothermal liquefaction of lignin in near-critical water in a new batch reactor: Influence of phenol and temperature. J. Supercrit. Fluids 123: 28–39. https://doi.org/10.1016/j.supflu.2016.12.015

Balakshin, M.Y., Capanema, E.A., Sulaeva, I., Schlee, P., Huang, Z., Feng, M., Borghei, M., Rojas, O.J., Potthast,

A. and Rosenau, T. (2021). New Opportunities in the Valorization of Technical Lignins. ChemSusChem 14: 1016–1036. https://doi.org/10.1002/cssc.202002553

Belkheiri, T. (2018). Hydrothermal liquefaction of lignin in sub-critical water to produce biofuel and chemicals. Doktorsavhandlingar vid Chalmers tekniska högskola. Ny serie: 4384. Chalmers University of Technology.

Belkheiri, T., Andersson, S.-I., Mattsson, C., Olausson, L., Theliander, H. and Vamling, L. (2018a). Hydrothermal Liquefaction of Kraft Lignin in Subcritical Water: Influence of Phenol as Capping Agent. Energy & Fuels 32: 5923–5932. https://doi.org/10.1021/acs.energyfuels.8b00068

Belkheiri, T., Andersson, S.-I., Mattsson, C., Olausson, L., Theliander, H. and Vamling, L. (2018b). Hydrothermal liquefaction of kraft lignin in sub-critical water: the influence of the sodium and potassium fraction. Biomass Convers. Biorefinery 8: 585–595. https://doi.org/10.1007/s13399-018-0307-9

Belkheiri, T., Mattsson, C., Andersson, S.I., Olausson, L., Åmand, L.E., Theliander, H. and Vamling, L. (2016). Effect of pH on Kraft Lignin Depolymerisation in Subcritical Water. Energy and Fuels 30: 4916–4924. https://doi.org/10.1021/acs.energyfuels.6b00462

Belkheiri, T., Vamling, L., Nguyen, T.D.H., Maschietti, M., Olausson, L., Andersson, S.-I., Åmand, L.-E. and Theliander, H. (2014). Kraft lignin depolymerization in near-critical water: effect of changing co-solvent. Cellul. Chem. Technol. 48: 813–818.

Berlin, A. and Balakshin, M. (2014). Industrial Lignins: Analysis, Properties, and Applications. In: Gupta, V.K., Tuohy, M.G., Kubicek, C.P., Saddler, J., and Xu, F. (Eds.). *Bioenergy Research: Advances and Applications*. Elsevier, Amsterdam, pp. 315–336. https://doi.org/10.1016/B978-0-444-59561-4.00018-8

Bobleter, O. and Concin, R. (1979). Degradation of poplar lignin by hydrothermal treatment. Cellul. Chem. Technol. 13: 583–593.

Brand, S., Hardi, F., Kim, J. and Suh, D.J. (2014). Effect of heating rate on biomass liquefaction: Differences between subcritical water and supercritical ethanol. Energy 68: 420–427. https://doi.org/10.1016/j.energy.2014.02.086

Bruijnincx, P., Weckhuysen, B., Gruter, G.-J. and Engelen-Smeets, E. (2016). Lignin valorisation : the importance of a full value chain approach. Utrecht.

Cao, L., Yu, I.K.M., Liu, Y., Ruan, X., Tsang, D.C.W., Hunt, A.J., Ok, Y.S., Song, H. and Zhang, S. (2018). Lignin valorization for the production of renewable chemicals: State-of-the-art review and future prospects. Bioresour. Technol. 269: 465–475. https://doi.org/10.1016/j.biortech.2018.08.065

Castello, D., Pedersen, T.H. and Rosendahl, L.A. (2018). Continuous hydrothermal liquefaction of biomass: A critical review. Energies 11: 3165. https://doi.org/10.3390/en11113165

Castello, D. and Rosendahl, L. (2018). Coprocessing of pyrolysis oil in refineries. In: Rosendahl, Lasse (Ed.). *Direct Thermochemical Liquefaction for Energy Applications*. Woodhead Publishing, pp. 293–317. https://doi.org/https://doi.org/10.1016/B978-0-08-101029-7.00008-4

Cheng, S., Wilks, C., Yuan, Z., Leitch, M. and Xu, C. (Charles) (2012). Hydrothermal degradation of alkali lignin to bio-phenolic compounds in sub/supercritical ethanol and water-ethanol co-solvent. Polym. Degrad. Stab. 97: 839–848. https://doi.org/10.1016/j.polymdegradstab.2012.03.044

Cheng, Y., Zhou, Z., Alma, M.H., Sun, D., Zhang, W. and Jiang, J. (2016). Direct liquefaction of alkali lignin in methanol and water mixture for the production of oligomeric phenols and aromatic ethers. J. Biobased Mater. Bioenergy 10: 76–80. https://doi.org/10.1166/jbmb.2016.1572

Deepa, A.K. and Dhepe, P.L. (2014). Solid acid catalyzed depolymerization of lignin into value added aromatic monomers. RSC Adv. 4: 12625–12629. https://doi.org/10.1039/c3ra47818a

Dessbesell, L., Paleologou, M., Leitch, M., Pulkki, R. and Xu, C. (Charles) (2020). Global lignin supply overview and kraft lignin potential as an alternative for petroleum-based polymers. Renew. Sustain. Energy Rev. 123: 109768. https://doi.org/10.1016/j.rser.2020.109768

Dimmel, D. (2010). Overview. In: Heiter, C., Dimmel, D.R., and Schmidt, J.A. (Eds.). *Lignins and Lignans Advances in Chemistry*. CRC Press, Boca Raton, pp. 1–9. https://doi.org/10.1017/CBO9781107415324.004

Dunn, K.G. and Hobson, P.A. (2016). Hydrothermal liquefaction of lignin. In: O'Hara, I., and Mundree, S. (Eds.). *Sugarcane-Based Biofuels and Bioproducts*. John Wiley & Sons, Inc., Hoboken, New Jersey, pp. 165–206.

Faix, O. (1992). Fourier transform infrared spectroscopy. In: Lin, S.Y., and Dence, C.W. (Eds.). *Methods in Lignin Chemistry*. Springer Science & Business Media, Berlin, pp. 83–109.

FAO (2021). Forestry Production and Trade [WWW Document]. FAOSTAT Food Agric. Organ. United Nations. URL https://www.fao.org/faostat/en/#data/FO (accessed 2.9.23).

Gellerstedt, G. (2015). Softwood kraft lignin: Raw material for the future. Ind. Crops Prod. 77: 845–854. https://doi.org/10.1016/j.indcrop.2015.09.040

Gellerstedt, G. (2009). Chemistry of Chemical Pulping. In: Ek, M., Gellerstedt, G., and Henriksson, G. (Eds.). *Pulp and Paper Chemistry and Technology Volume 2 Pulping Chemistry and Technology*. De Gruyter, Berlin, Boston, pp. 91–120.

Gellerstedt, G. and Henriksson, G. (2008). Lignins: Major Sources, Structure and Properties. In: Belgacem, M.N., and Gandini, A. (Eds.). *Monomers, Polymers and Composites from Renewable Resources*. Elsevier, Amsterdam, pp. 201–224. https://doi.org/https://doi.org/10.1016/B978-0-08-045316-3.00009-0

Gellerstedt, G., Majtnerova, A. and Zhang, L. (2004). Towards a new concept of lignin condensation in kraft pulping. Initial results. Comptes Rendus - Biol. 327: 817–826. https://doi.org/10.1016/j.crvi.2004.03.011

Gellerstedt, G., Tomani, P., Axegård, P. and Backlund, B. (2013). Lignin recovery and lignin-based products. In: Christopher, L. (Ed.). *Integrated Forest Biorefineries–Challenges and Opportunities*. Royal Society of Chemistry, Cambridge, pp. 180–210.

Giummarella, N., Lindén, P.A., Areskogh, D. and Lawoko, M. (2020). Fractional Profiling of Kraft Lignin Structure: Unravelling Insights on Lignin Reaction Mechanisms. ACS Sustain. Chem. Eng. 8: 1112–1120. https://doi.org/10.1021/acssuschemeng.9b06027

Gosselink, R.J.A., Teunissen, W., van Dam, J.E.G., de Jong, E., Gellerstedt, G., Scott, E.L. and Sanders, J.P.M. (2012). Lignin depolymerisation in supercritical carbon dioxide/acetone/water fluid for the production of aromatic chemicals. Bioresour. Technol. 106: 173–177. https://doi.org/10.1016/j.biortech.2011.11.121

Guo, M., Maltari, R., Zhang, R., Kontro, J., Ma, E. and Repo, T. (2021). Hydrothermal Depolymerization of Kraft Lignins with Green C1-C3Alcohol-Water Mixtures. Energy and Fuels 35: 15770–15777. https://doi.org/10.1021/acs.energyfuels.1c01968

Han, Y., Hoekman, K., Jena, U. and Das, P. (2020). Use of co-solvents in hydrothermal liquefaction (HTL) of microalgae. Energies 13:. https://doi.org/10.3390/en13010124

Henriksson, G. (2009). Lignin. In: Ek, M., Gellerstedt, G., and Henriksson, G. (Eds.). *Pulp and Paper Chemistry and Technology Volume 1 Wood Chemistry and Wood Biotechnology*. Walter de Gruyter GmbH & Co. KG, Berlin, pp. 121–146.

Henriksson, G., Brännvall, E. and Lennholm, H. (2009). The Trees. In: Ek, M., Gellerstedt, G., and Henriksson, G. (Eds.). *Wood Chemistry and Biotechnology Volume 1 Wood Chemistry and Wood Biotechnology*. Walter de Gruyter GmbH & Co. KG, Berlin, pp. 13–44.

Jensen, A., Nielsen, J.B., Jensen, A.D. and Felby, C. (2018). Chapter 4: Thermal and Solvolytic Depolymerization Approaches for Lignin Depolymerization and Upgrading. In: Beckham, G.T. (Ed.). *Lignin Valorization: Emerging Approaches*. The Royal Society of Chemistry, Cambridge, UK, pp. 74–107. https://doi.org/10.1039/9781788010351-00074

Kashimalla, M., Suraboyina, S., Dubbaka, V. and Polumati, A. (2021). Optimisation of a catalytic hydrothermal liquefaction process using central composite design for yield improvement of bio-oil. Biomass Convers. Biorefinery 1–13. https://doi.org/10.1007/s13399-021-01451-8

Kim, K.H., Brown, R.C., Kieffer, M. and Bai, X. (2014). Hydrogen-donor-assisted solvent liquefaction of lignin to short-chain alkylphenols using a micro reactor/gas chromatography system. Energy and Fuels 28: 6429–6437. https://doi.org/10.1021/ef501678w

Kruse, A. and Dahmen, N. (2015). Water - A magic solvent for biomass conversion. J. Supercrit. Fluids 96: 36–

45. https://doi.org/10.1016/j.supflu.2014.09.038

Lancefield, C.S., Wienk, H.J., Boelens, R., Weckhuysen, B.M. and Bruijnincx, P.C.A. (2018). Identification of a diagnostic structural motif reveals a new reaction intermediate and condensation pathway in kraft lignin formation. Chem. Sci. 9: 6348–6360. https://doi.org/10.1039/c8sc02000k

Lange, J. (2015). Renewable Feedstocks: The Problem of Catalyst Deactivation and its Mitigation. Angew. Chemie Int. Ed. 54: 13186–13197. https://doi.org/10.1002/ange.201503595

Lappalainen, J., Baudouin, D., Hornung, U., Schuler, J., Melin, K., Bjelić, S., Vogel, F., Konttinen, J. and Joronen, T. (2020). Sub- and Supercritical Water Liquefaction of Kraft Lignin and Black Liquor Derived Lignin. Energies 13: 3309. https://doi.org/10.3390/en13133309

Lawoko, M. and Samec, J.S.M. (2023). Kraft lignin valorization: Biofuels and thermoset materials in focus. Curr. Opin. Green Sustain. Chem. 40: 100738. https://doi.org/10.1016/j.cogsc.2022.100738

Lawson, J.R. and Klein, M.T. (1985). Influence of water on guaiacol pyrolysis. Ind. Eng. Chem. Fundam. 24: 203–208.

Lee, H.-S., Jae, J., Ha, J.-M. and Suh, D.J. (2016). Hydro- and solvothermolysis of kraft lignin for maximizing production of monomeric aromatic chemicals. Bioresour. Technol. 203: 142–149. https://doi.org/10.1016/j.biortech.2015.12.022

Löfstedt, J., Dahlstrand, C., Orebom, A., Meuzelaar, G., Sawadjoon, S., Galkin, M. V., Agback, P., Wimby, M., Corresa, E., Mathieu, Y., Sauvanaud, L., Eriksson, S., Corma, A. and Samec, J.S.M. (2016). Green Diesel from Kraft Lignin in Three Steps. ChemSusChem 9: 1392–1396. https://doi.org/10.1002/cssc.201600172

Lora, J. (2008). Industrial Commercial Lignins: Sources, Properties and Applications. In: Belgacem, M.N., and Gandini, A. (Eds.). *Monomers, Polymers and Composites from Renewable Resources*. Elsevier, Amsterdam, pp. 225–241. https://doi.org/https://doi.org/10.1016/B978-0-08-045316-3.00010-7

Mattsson, C., Andersson, S.I., Belkheiri, T., Åmand, L.E., Olausson, L., Vamling, L. and Theliander, H. (2016). Using 2D NMR to characterize the structure of the low and high molecular weight fractions of bio-oil obtained from LignoBoost^{TM} kraft lignin depolymerized in subcritical water. Biomass and Bioenergy 95: 364–377. https://doi.org/10.1016/j.biombioe.2016.09.004

McCarthy, J.L. and Islam, A. (2000). Lignin chemistry, technology, and utilization: a brief history. In: Glasser, W.G., Northey, R.A., and Schultz, T.P. (Eds.). *Lignin: Historical, Biological, and Materials Perspectives*. ACS Publications, pp. 2–99.

McClelland, D.J., Motagamwala, A.H., Li, Y., Rover, M.R., Wittrig, A.M., Wu, C., Buchanan, J.S., Brown, R.C., Ralph, J., Dumesic, J.A. and Huber, G.W. (2017). Functionality and molecular weight distribution of red oak lignin before and after pyrolysis and hydrogenation. Green Chem. 19: 1378–1389. https://doi.org/10.1039/c6gc03515a

Miller, J.E., Evans, L., Littlewolf, A. and Trudell, D.E. (1999). Batch microreactor studies of lignin and lignin model compound depolymerization by bases in alcohol solvents, Fuel. https://doi.org/10.1016/S0016-2361(99)00072-1

Miller, J.E., Evans, L., Mudd, J.E. and Brown, K.A. (2002). Batch Microreactor Studies of Lignin Depolymerization by Bases. 2. Aqueous Solvents, Sandia National Laboratories Report, SAND2002-1318. https://doi.org/10.2172/800964

Mottiar, Y., Vanholme, R., Boerjan, W., Ralph, J. and Mansfield, S.D. (2016). Designer lignins: Harnessing the plasticity of lignification. Curr. Opin. Biotechnol. 37: 190–200. https://doi.org/10.1016/j.copbio.2015.10.009

Nguyen, T.D.H., Maschietti, M., Åmand, L.E., Vamling, L., Olausson, L., Andersson, S.I. and Theliander, H. (2014a). The effect of temperature on the catalytic conversion of Kraft lignin using near-critical water. Bioresour. Technol. 170: 196–203. https://doi.org/10.1016/j.biortech.2014.06.051

Nguyen, T.D.H., Maschietti, M., Belkheiri, T., Åmand, L.E., Theliander, H., Vamling, L., Olausson, L. and Andersson, S.I. (2014b). Catalytic depolymerisation and conversion of Kraft lignin into liquid products using near-critical water. J. Supercrit. Fluids 86: 67–75. https://doi.org/10.1016/j.supflu.2013.11.022

Okuda, K., Umetsu, M., Takami, S. and Adschiri, T. (2004). Disassembly of lignin and chemical recovery - Rapid depolymerization of lignin without char formation in water-phenol mixtures. Fuel Process. Technol. 85: 803–813. https://doi.org/10.1016/j.fuproc.2003.11.027

Otromke, M., Shuttleworth, P.S., Sauer, J. and White, R.J. (2019a). Hydrothermal base catalysed treatment of Kraft Lignin for the preparation of a sustainable carbon fibre precursor. Bioresour. Technol. Reports 5: 251–260. https://doi.org/10.1016/j.biteb.2018.11.001

Otromke, M., Shuttleworth, P.S., Sauer, J. and White, R.J. (2019b). Hydrothermal base catalysed treatment of Kraft lignin - time dependent analysis and a techno-economic evaluation for carbon fibre applications. Bioresour. Technol. Reports 6: 241–250. https://doi.org/10.1016/j.biteb.2019.03.008

Otromke, M., White, R.J. and Sauer, J. (2019c). Hydrothermal base catalyzed depolymerization and conversion of technical lignin – An introductory review. Carbon Resour. Convers. 2: 59–71. https://doi.org/10.1016/j.crcon.2019.01.002

Pandey, M.P. and Kim, C.S. (2011). Lignin Depolymerization and Conversion: A Review of Thermochemical Methods. Chem. Eng. Technol. 34: 29–41. https://doi.org/10.1002/ceat.201000270

Pedersen, T.H., Grigoras, I.F., Hoffmann, J., Toor, S.S., Daraban, I.M., Jensen, C.U., Iversen, S.B., Madsen, R.B., Glasius, M., Arturi, K.R., Nielsen, R.P., Søgaard, E.G. and Rosendahl, L.A. (2016). Continuous hydrothermal co-liquefaction of aspen wood and glycerol with water phase recirculation. Appl. Energy 162: 1034–1041. https://doi.org/10.1016/j.apenergy.2015.10.165

Pedersen, T.H., Jasiunas, L., Casamassima, L., Singh, S., Jensen, T. and Rosendahl, L.A. (2015). Synergetic hydrothermal co-liquefaction of crude glycerol and aspen wood. Energy Convers. Manag. 106: 886–891. https://doi.org/10.1016/j.enconman.2015.10.017

Pérez, E., Abad-Fernández, N., Lourençon, T., Balakshin, M., Sixta, H. and Cocero, M.J. (2022). Base-catalysed depolymerization of lignins in supercritical water: Influence of lignin nature and valorisation of pulping and biorefinery by-products. Biomass and Bioenergy 163:. https://doi.org/10.1016/j.biombioe.2022.106536

Peterson, A.A., Vogel, F., Lachance, R.P., Fröling, M., Antal, M.J. and Tester, J.W. (2008). Thermochemical biofuel production in hydrothermal media: A review of sub- and supercritical water technologies. Energy Environ. Sci. 1: 32–65. https://doi.org/10.1039/b810100k

Rabinovich, M.L. (2010). Wood hydrolysis industry in the soviet union and Russia: A mini-review. Cellul. Chem. Technol. 44: 173–186.

Ragauskas, A.J., Beckham, G.T., Biddy, M.J., Chandra, R., Chen, F., Davis, M.F., Davison, B.H., Dixon, R.A., Gilna, P., Keller, M., Langan, P., Naskar, A.K., Saddler, J.N., Tschaplinski, T.J., Tuskan, G.A. and Wyman, C.E. (2014). Lignin valorization: Improving lignin processing in the biorefinery. Science (80-.). 344:. https://doi.org/10.1126/science.1246843

Roberts, V.M., Stein, V., Reiner, T., Lemonidou, A., Li, X. and Lercher, J.A. (2011). Towards quantitative catalytic lignin depolymerization. Chem. - A Eur. J. 17: 5939–5948. https://doi.org/10.1002/chem.201002438

Ross, D.S. and Blessing, J.E. (1979). Alcohols as H-donor media in coal conversion. 2. Base-promoted H-donation to coal by methyl alcohol. Fuel 58: 438–442. https://doi.org/10.1016/0016-2361(79)90085-1

Rößiger, B., Röver, R., Unkelbach, G. and Pufky-Heinrich, D. (2017). Production of Bio-Phenols for Industrial Application: Scale-Up of the Base-Catalyzed Depolymerization of Lignin. Green Sustain. Chem. 7: 193–202. https://doi.org/10.4236/gsc.2017.73015

Rößiger, B., Unkelbach, G. and Pufky-Heinrich, D. (2018). Base-catalyzed depolymerization of lignin: History, challenges and perspectives. In: Poletto, M. (Ed.). *Lignin - Trends and Applications*. IntechOpen, London, UK, London, pp. 99–120. https://doi.org/10.5772/intechopen.68464

Saake, B. and Lehnen, R. (2007). Lignin. In: *Ullmann's Encyclopedia of Industrial Chemistry*. John Wiley & Sons, Ltd. https://doi.org/https://doi.org/10.1002/14356007.a15_305.pub3

Saisu, M., Sato, T., Watanabe, M., Adschiri, T. and Arai, K. (2003). Conversion of lignin with supercritical water-phenol mixtures. Energy & Fuels 17: 922–928. https://doi.org/10.1021/ef0202844

Sato, T., Sekiguchi, G., Adschiri, T. and Arai, K. (2002). Ortho-selective alkylation of phenol with 2-propanol without catalyst in supercritical water. Ind. Eng. Chem. Res. 41: 3064–3070. https://doi.org/10.1021/ie0200712

Schmiedl, D., Endisch, S., Pindel, E., Rückert, D., Reinhardt, S., Schweppe, R. and Unkelbach, G. (2012). Base catalyzed degradation of Lignin for the generation of oxy-aromatic compounds - Possibilities and challenges. Erdöl Erdgas Kohle 128: 357–363.

Schutyser, W., Renders, T., Van Den Bosch, S., Koelewijn, S.F., Beckham, G.T. and Sels, B.F. (2018). Chemicals from lignin: An interplay of lignocellulose fractionation, depolymerisation, and upgrading. Chem. Soc. Rev. 47: 852–908. https://doi.org/10.1039/c7cs00566k

Subbotina, E., Rukkijakan, T., Marquez-Medina, M.D., Yu, X., Johnsson, M. and Samec, J.S.M. (2021). Oxidative cleavage of C–C bonds in lignin. Nat. Chem. 13: 1118–1125. https://doi.org/10.1038/s41557-021-00783-2

Sulaeva, I., Zinovyev, G., Plankeele, J.M., Sumerskii, I., Rosenau, T. and Potthast, A. (2017). Fast Track to Molar-Mass Distributions of Technical Lignins. ChemSusChem 10: 629–635. https://doi.org/10.1002/cssc.201601517

Theliander, H. (2008). Withdrawing lignin from black liquor by precipitation, filtration and washing. In: *2008 Nordic Wood Biorefinery Conference, March 11-14, Stockholm, Sweden*.

Toledano, A., Serrano, L. and Labidi, J. (2014). Improving base catalyzed lignin depolymerization by avoiding lignin repolymerization. Fuel 116: 617–624. https://doi.org/https://doi.org/10.1016/j.fuel.2013.08.071

Toor, S.S., Rosendahl, L. and Rudolf, A. (2011). Hydrothermal liquefaction of biomass: A review of subcritical water technologies. Energy 36: 2328–2342. https://doi.org/10.1016/j.energy.2011.03.013

Tsujino, J., Kawamoto, H. and Saka, S. (2003). Reactivity of lignin in supercritical methanol studied with various lignin model compounds. Wood Sci. Technol. 37: 299–307. https://doi.org/10.1007/s00226-003-0187-3

Umar, Y., Velasco, O., Abdelaziz, O.Y., Aboelazayem, O., Gadalla, M.A., Hulteberg, C.P. and Saha, B. (2022). A renewable lignin-derived bio-oil for boosting the oxidation stability of biodiesel. Renew. Energy 182: 867–878. https://doi.org/10.1016/j.renene.2021.10.061

Wahyudiono, Kanetake, T., Sasaki, M. and Goto, M. (2007). Decomposition of a lignin model compound under hydrothermal conditions. Chem. Eng. Technol. 30: 1113–1122. https://doi.org/10.1002/ceat.200700066

Wahyudiono, Sasaki, M. and Goto, M. (2011). Thermal decomposition of guaiacol in sub- and supercritical water and its kinetic analysis. J. Mater. Cycles Waste Manag. 13: 68–79. https://doi.org/10.1007/s10163-010-0309-6

Wahyudiono, Sasaki, M. and Goto, M. (2008). Recovery of phenolic compounds through the decomposition of lignin in near and supercritical water. Chem. Eng. Process. Process Intensif. 47: 1609–1619. https://doi.org/10.1016/j.cep.2007.09.001

Ye, Y., Fan, J. and Chang, J. (2012a). Effect of reaction conditions on hydrothermal degradation of cornstalk lignin. J. Anal. Appl. Pyrolysis 94: 190–195. https://doi.org/10.1016/j.jaap.2011.12.005

Ye, Y., Zhang, Y., Fan, J. and Chang, J. (2012b). Novel method for production of phenolics by combining lignin extraction with lignin depolymerization in aqueous ethanol. Ind. Eng. Chem. Res. 51: 103–110. https://doi.org/10.1021/ie202118d

Yong, T.L.K. and Matsumura, Y. (2013). Kinetic analysis of lignin hydrothermal conversion in sub- and supercritical water. Ind. Eng. Chem. Res. 52: 5626–5639. https://doi.org/10.1021/ie400600x

Yong, T.L.K. and Matsumura, Y. (2012). Reaction kinetics of the lignin conversion in supercritical water. Ind. Eng. Chem. Res. 51: 11975–11988. https://doi.org/10.1021/ie300921d

Yong, T.L.K. and Yukihiko, M. (2013). Kinetic analysis of guaiacol conversion in sub- and supercritical water. Ind. Eng. Chem. Res. 52: 9048–9059. https://doi.org/10.1021/ie4009748

Yu, X., Wei, Z., Lu, Z., Pei, H. and Wang, H. (2019). Activation of lignin by selective oxidation: An emerging strategy for boosting lignin depolymerization to aromatics. Bioresour. Technol. 291: 121885. https://doi.org/10.1016/j.biortech.2019.121885

Yuan, X.Z., Li, H., Zeng, G.M., Tong, J.Y. and Xie, W. (2007). Sub- and supercritical liquefaction of rice straw in the presence of ethanol-water and 2-propanol-water mixture. Energy 32: 2081–2088. https://doi.org/10.1016/j.energy.2007.04.011

Zakzeski, J., Bruijnincx, P.C.A., Jongerius, A.L. and Weckhuysen, B.M. (2010). The Catalytic Valorization of Lignin for the Production of Renewable Chemicals. Chem. Rev. 110: 3552–3599. https://doi.org/10.1021/cr900354u

Zhang, B., Huang, H.J. and Ramaswamy, S. (2008). Reaction kinetics of the hydrothermal treatment of lignin. Appl. Biochem. Biotechnol. 147: 119–131. https://doi.org/10.1007/s12010-007-8070-6

Zhu, W., Westman, G. and Theliander, H. (2014). Investigation and characterization of lignin precipitation in the lignoboost process. J. Wood Chem. Technol. 34: 77–97. https://doi.org/10.1080/02773813.2013.838267

Zinovyev, G., Sulaeva, I., Podzimek, S., Rössner, D., Kilpeläinen, I., Sumerskii, I., Rosenau, T. and Potthast, A. (2018). Getting Closer to Absolute Molar Masses of Technical Lignins. ChemSusChem 11: 3259–3268. https://doi.org/10.1002/cssc.201801177

Appendix I - Reaction temperature and pressure profiles

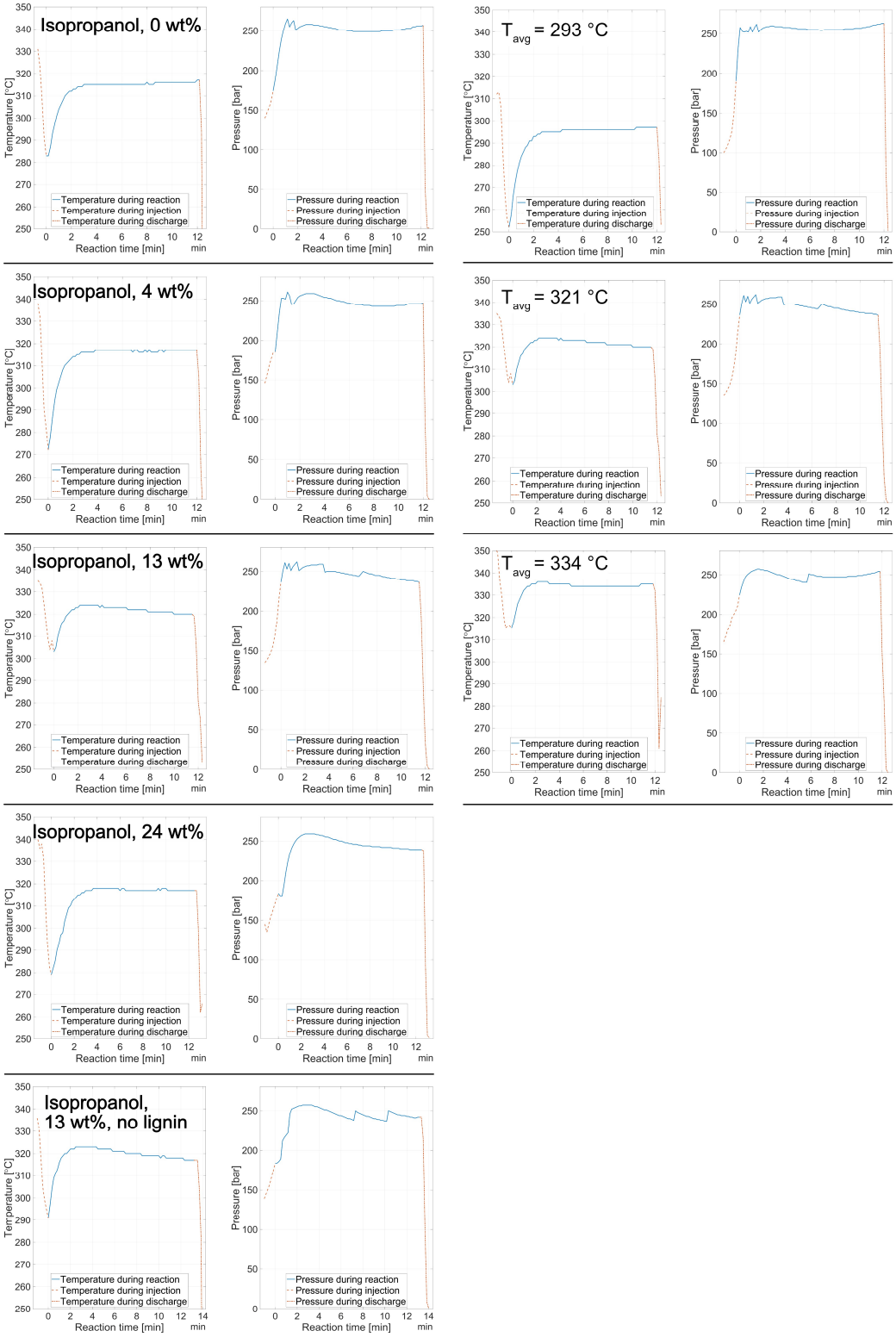

Figure A1: Temperature and pressure profiles in the reactor during injection, reaction and ejection in Paper I.

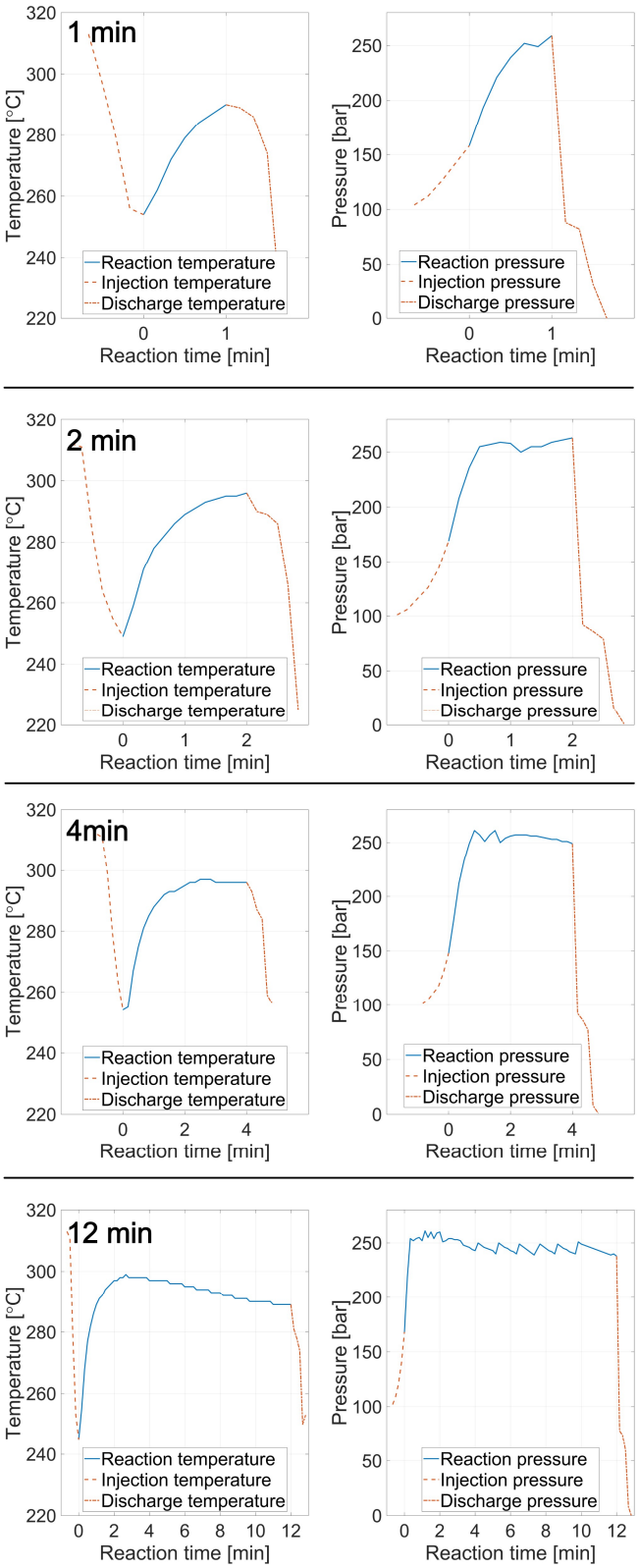

Figure A2: Temperature and pressure profiles in the reactor during injection, reaction, and ejection in Paper II.

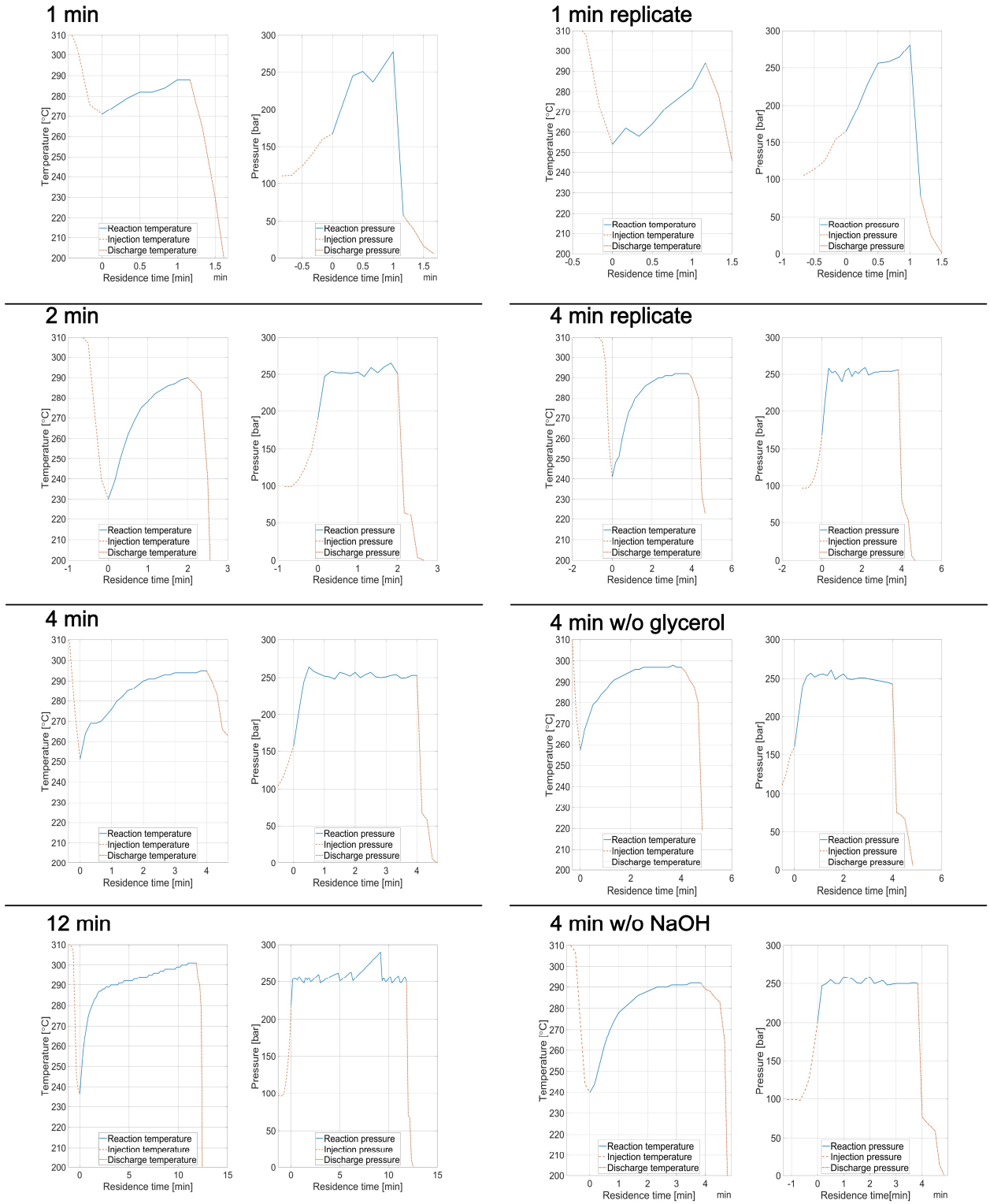

Figure A3: Temperature and pressure profiles in the reactor during injection, reaction, and ejection in Paper III.

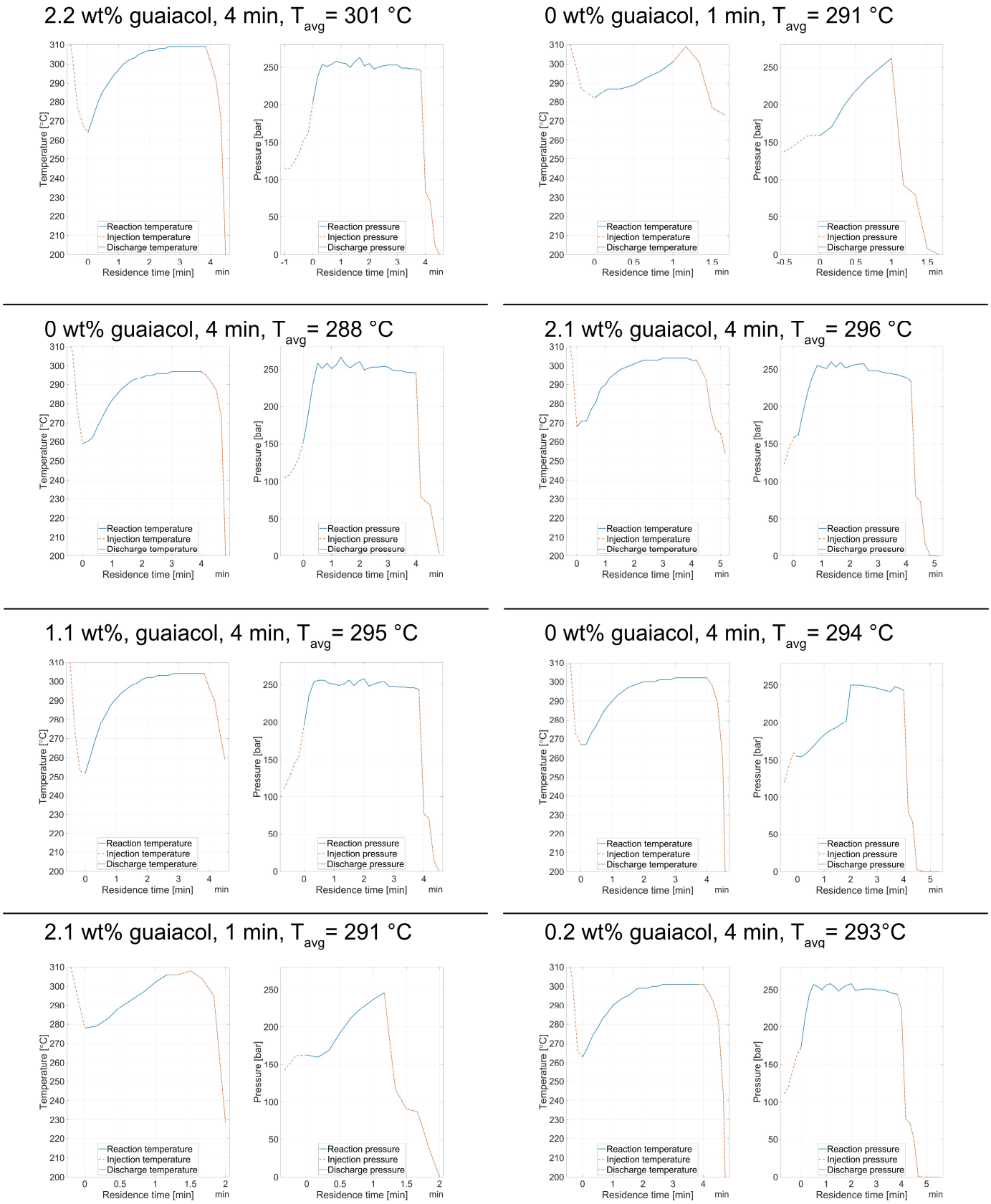

Figure A4: Temperature and pressure profiles in the reactor during injection, reaction, and ejection in Paper IV.

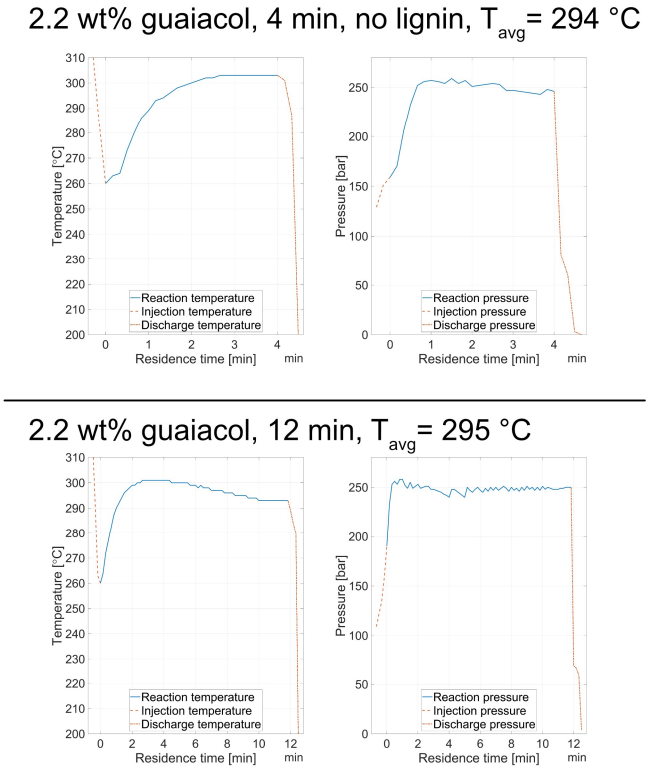

Figure A5: Temperature and pressure profiles in the reactor during injection, reaction, and ejection in Paper IV.

Appendix II – Diphenylmethanes

Aliphatic regions of HSQC spectra for LignoBoost lignin and PS are presented in Figure A6 with regions associated with diphenylmethanes marked with black rectangles (Adamovic *et al.* 2022).

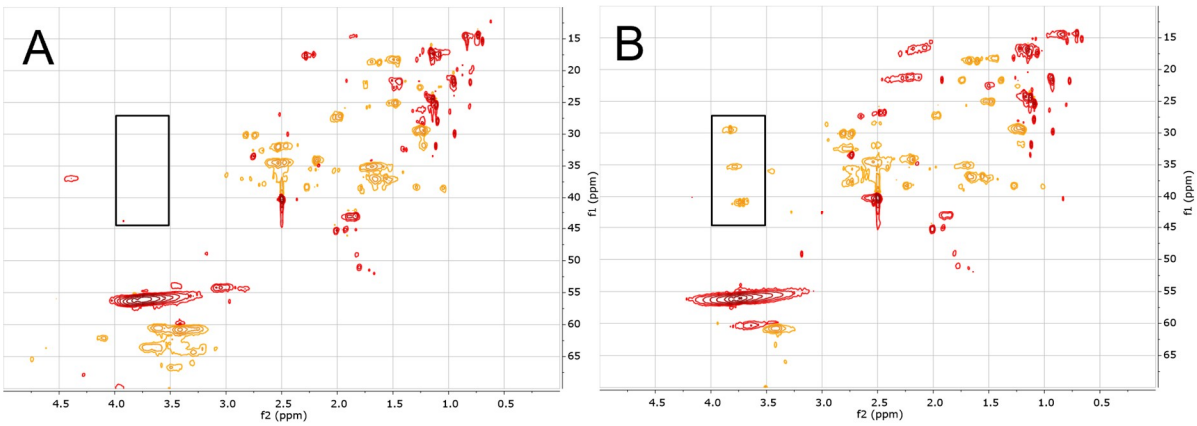

Figure A6: Aliphatic region of HSQC spectra from the study from Paper IV. LignoBoost (A) and PS run for 12 min at T_{avg} = 295 °C with 2.2 wt% guaiacol added. Diphenylmethane peaks are marked with a black rectangle (Adamovic et al. 2022).